



# **Simulation of production process-related adhesive damage of adhesively bonded multi-material body in white**

## **Studienarbeit**

Name: Suba Siva Chandran Kalimuthu  
Matriculation Number: 4868941  
Course: Computational Sciences in Engineering

Examiner: Univ.-Prof. Dr.-Ing. Prof.h.c. Klaus Dilger

Supervisor: Niklas Günther M.Sc.,  
Institut für Füge und Schweißtechnik

In cooperation with: GNS mbH  
Crash simulation - Research and Methods

Company supervisor: Dipl.-Ing. Erdeniz Ince

Date of Submission: 11.05.2020

# **Declaration**

I hereby declare on oath that I have independently written the present Student work "Simulation of production process-related adhesive damage of adhesively bonded multi-material body in white" and I have fully stated all sources and tools used. The work has not been submitted as an examination paper before.

Braunschweig, 11.05.2020

Signature

---

# Abstract

Due to ever increasing vehicle weights and crash requirements, bodies with multi-material construction have been developed in recent years. During the manufacturing process of such vehicles, the body in white undergoes a painting process for corrosion protection, which is referred to as cathodic dip painting. Temperatures around 185 °C prevail in the dryer after the cataphoretic dip coating process. Due to the different thermal expansion coefficients of a multi-material structure, the adhesive layer can be damaged and the sheets can be warped during the manufacturing process. In order to identify them as early as possible and if possible to prevent them, it is necessary to look into the damage in the adhesive layer using FEM.

In this work, the vehicle model of Toyota Camry already available at GNS mbH is used to investigate how the thermal expansion of different materials affects the damage to an adhesive layer in a real geometry. The present vehicle model available at GNS mbH has to be converted to a working model in ABAQUS™. Using this calculation model, the temperatures within transient heat transfer analysis should be calculated first and then it should be used in a second step to determine the displacements and adhesive damage. For simulating the adhesive layer stress, the bilinear temperature-dependent cohesive zone model available to GNS mbH is used for a fully cured adhesive.

# Contents

<b>List of Abbreviations</b>	<b>IV</b>
<b>List of Figures</b>	<b>V</b>
<b>List of Tables</b>	<b>VII</b>
<b>List of Variables</b>	<b>VIII</b>
<b>1 Introduction</b>	<b>1</b>
<b>2 State of the art</b>	<b>3</b>
2.1 Cathodic dip painting . . . . .	3
2.2 Adhesives in vehicle body construction . . . . .	4
2.3 Delta Alpha problem during the paint-dryer process . . . . .	5
2.4 Adhesive problems during the paint-dryer process . . . . .	8
<b>3 Workflow of the simulation of cooling process</b>	<b>9</b>
3.1 ANSA™ preprocessor . . . . .	10
3.1.1 Connection manager . . . . .	10
3.1.2 Working with connection manager . . . . .	11
3.1.3 Surface set definition for Steel and Aluminium . . . . .	14
3.2 ABAQUS™ FE solver . . . . .	15
3.2.1 Thermo-Mechanical analysis . . . . .	16
3.2.2 Sequentially coupled thermal-stress analysis . . . . .	16
<b>4 Material model validation</b>	<b>18</b>
4.1 Steel hatprofile . . . . .	18
4.1.1 Experimental procedure of Steel hatprofile . . . . .	19
4.1.2 Simulation of Steel hatprofile . . . . .	20
4.2 Aluminium plate . . . . .	24
4.2.1 Experimental procedure of Aluminium plate . . . . .	24
4.2.2 Simulation of Aluminium plate . . . . .	25
4.3 Combined Steel and Aluminium profiles with shell elements . . . . .	27
4.3.1 Combined shell model description . . . . .	27
4.3.2 Description of the adhesive used . . . . .	28
4.3.3 Thermal analysis of combined shell model . . . . .	31
4.3.4 Mechanical analysis of combined shell model . . . . .	33
<b>5 FEM simulation on the vehicle model</b>	<b>36</b>
5.1 Description of the model . . . . .	36
5.2 Brief discussion on Toyota Camry model . . . . .	36

5.3 Thermal and Mechanical analysis of the vehicle structure . . . . .	38
<b>6 Observation and Results</b>	<b>39</b>
<b>7 Objections confronted</b>	<b>47</b>
<b>8 Summary</b>	<b>49</b>
<b>9 Bibliography</b>	<b>IX</b>

# List of Abbreviations

Abbreviation	Description
TM	Trade Mark
EU	European Union
FEM	Finite Element Method
FEA	Finite Element Analysis
BIW	Body-in-White
CDC	Cataphoretic dip coating
BM	Betamate
KTL	Kathodische Tauchlackierung
GNS	Gesellschaft für numerische Simulation
EDP	Electrophoretic deposition
CDP	Cathodic dip painting
CAE	Computer-aided engineering
ANSA	Automatic net generation for structural analysis
CAD	Computer-aided design
TIC	Thermal imaging camera
MPC	Multi-point constraint
TU	Technische Universität

# List of Figures

Figure 2.1	Cathodic dip painting of a vehicle body [1] . . . . .	3
Figure 2.2	Schematic representation of cathodic dip painting process . . . . .	4
Figure 2.3	Paint drying oven [2] . . . . .	5
Figure 2.4	Scope of adhesive in modern BIW [3] . . . . .	6
Figure 2.5	Types of Adhesive damage . . . . .	7
Figure 3.1	Phases in the simulation of cooling process . . . . .	9
Figure 3.2	Top and side views of the Camry model . . . . .	10
Figure 3.3	Connection manager tool in ANSA™ [4] . . . . .	11
Figure 3.4	PLINKS in PAM-CRASH™ database . . . . .	12
Figure 3.5	Selection of PLINKS . . . . .	13
Figure 3.6	Conversion of PLINKS to connection points . . . . .	13
Figure 3.7	Change to suitable FE representation type in connection manager . . . . .	14
Figure 3.8	Conversion of PLINKS to suitable FE representation type in ABAQUS™ . . . . .	14
Figure 3.9	Surface set creation for Aluminium part . . . . .	15
Figure 4.1	Experimental cooling process of DC01 Steel hatprofile . . . . .	18
Figure 4.2	DC01 Steel hatprofile . . . . .	19
Figure 4.3	Experimental cooling rate of the DC01 Steel hatprofile . . . . .	20
Figure 4.4	Dimensions of Steel hatprofile model in ABAQUS™ . . . . .	21
Figure 4.5	Temperature measurement points in ABAQUS™ for DC01 Steel . . . . .	22
Figure 4.6	Experiment 1 cooling rate vs Simulation 1 cooling rate for DC01 Steel . . . . .	22
Figure 4.7	Experiment 2 cooling rate vs Simulation 2 cooling rate for DC01 Steel . . . . .	23
Figure 4.8	Experiment 3 cooling rate vs Simulation 3 cooling rate for DC01 Steel . . . . .	23
Figure 4.9	Experimental cooling rate of the EN AW-6082-T6 Aluminium plate . . . . .	25
Figure 4.10	Dimensions of Aluminium plate model in ABAQUS™ . . . . .	25
Figure 4.11	Temperature measurement points in ABAQUS™ for EN AW-6082 Aluminium . . . . .	26
Figure 4.12	Experiment 1 cooling rate vs Simulation 1 cooling rate for EN AW-6082-T6 Aluminium . . . . .	27
Figure 4.13	A view of combined shell model . . . . .	28
Figure 4.14	Enlarged view of spot welds and adhesive in combined shell model . . . . .	29
Figure 5.1	Aluminium parts in the entire car model . . . . .	37
Figure 5.2	Aluminium flanges glued to the Steel platform . . . . .	37
Figure 5.3	Cohesive element type COS3D in PAM-CRASH™ [5] . . . . .	38

---

Figure 6.1	Temperature distribution after 527 seconds during cooling . . . . .	39
Figure 6.2	Temperature difference between thick and thin shell parts . . . . .	40
Figure 6.3	Measurement point to illustrate temperature difference . . . . .	40
Figure 6.4	Temperature difference of upper rail rear and top parts connected by spotweld . . . . .	41
Figure 6.5	Temperature distribution of Camry model after 2400 seconds . . . . .	41
Figure 6.6	Displacement of the Camry model after 280 seconds . . . . .	43
Figure 6.7	Displacement of the floor front during cooling . . . . .	43
Figure 6.8	Deformation of the aluminium flange . . . . .	44
Figure 6.9	Stiffness degradation of the adhesive in region of aluminium flange	44
Figure 6.10	Crossing of adhesives with spot weld . . . . .	45
Figure 6.11	SDEG results in B-pillar and rear outer panel . . . . .	45

# List of Tables

Table 2.1	Thermal expansion coefficients of Steel and Aluminium . . . . .	6
Table 4.1	Different room temperatures of the conducted experiments . . . . .	19
Table 4.2	Thermal properties used for DC01 Steel . . . . .	20
Table 4.3	Temperature-dependent film coefficients obtained from ABAQUS™	21
Table 4.4	Temperature-dependent film coefficients finalized for Steel material	24
Table 4.5	Thermal properties used for EN AW-6082-T6 Aluminium . . . . .	26
Table 4.6	Temperature dependent film coefficients obtained from ABAQUS™	26
Table 4.7	Thermal properties used for BETAMATE™ 1480V203 . . . . .	29
Table 4.8	Elastic properties used for BETAMATE™ 1480V203 . . . . .	29
Table 4.9	Thermal expansion coefficients used for BETAMATE™ 1480V203 .	30
Table 4.10	Damage initiation properties used for BETAMATE™ 1480V203 . .	30
Table 4.11	Damage evolution properties used for BETAMATE™ 1480V203 . .	30
Table 4.12	Heat transfer element types used for combined shell model . . . . .	32
Table 4.13	Elastic properties of DC01 Steel and EN AW-6082-T6 Aluminium .	33
Table 4.14	Plastic properties for DC01 Steel . . . . .	33
Table 4.15	Plastic properties for EN AW-6082-T6 Aluminium . . . . .	34
Table 4.16	Stress element types used for combined shell model . . . . .	35
Table 6.1	Comparitive time duration of the analysis jobs . . . . .	42

# List of Variables

Symbol	Property	Unit
$\alpha$	Coefficient of thermal expansion	$K^{-1}$
$\rho$	Density	$ton\ mm^{-3}$
$k$	Thermal conductivity	$mW\ mm^{-1}K^{-1}$
$c$	Specific heat capacity	$mJ\ ton^{-1}K^{-1}$

# 1 Introduction

Nowadays, mobility is one of the indispensable requirements of the people. The vehicles are an important means of transportation in day-to-day life. Ensuring mobility in future is a great challenge in addition to the social responsibility of an engineer. In this context, the automotive industries are undergoing some challenges to develop changes for the future. Due to the increasing environmental awareness of customers and strict laws, significant reductions in fuel consumption and a reduction in CO<sub>2</sub> emissions are expected. According to the draft of an EU guideline [6], a CO<sub>2</sub> limit value curve based on the vehicle weight is planned for new vehicles. According to this, the target is to emit no more than 120g CO<sub>2</sub> / km on average. A weight reduction of 100kg in the vehicle saves approx. 8.5g CO<sub>2</sub> / km, provided that the drive train and chassis are also adapted to the reduced weight.

In automotive engineering sector, new lightweight construction developments are being carried out in multi-material vehicle body construction. The newly developed construction methods also requires certain material adapted joining concepts. The use of adhesives for joining the multi-material parts is more advisable and convenient. The expectation of simulating these kind of manufacturing processes of different connections are high and plays an important role in product development process as it helps in significantly reducing development times, using increasing variety of variants, increasing the testing quality of prototypes and expanding testing options [7].

The structural adhesives such as hot curing epoxy resin adhesives are preferred for bonding the multi-material BIW structures due to their high strength [8]. The adhesives has to meet high thermal and mechanical stresses during the manufacturing process. During the drying process after CDC, the joining partners expands due to the thermal loads and also the different heat distributions prevailing in them. Depending on the dimension of parts to be joined, relative movements of several millimetres can occur. This leads to the stresses which might lead to the deformation in the adhesive layer. So, to become aware of the stresses in the adhesive layer, configuring the properties before hand is of great importance and could prevent the damages in the production stage. Therefore, taking into account the temperature-dependent adhesive properties is the basis of description and simulation of these kind of manufacturing-related deformations. In order to reduce the effort required for experiments, FEM simulations are increasingly being carried out. The calculation of adhesive bonds in car bodies during the paint-dryer process faces the challenge of extensive data models and long process times [7]. At the same time, high quality results are required to predict adhesive failure and component deformation.

As per the current state of the art, it is not possible to measure the stresses in multi-material BIW construction with the thermosetting adhesives due to the delta alpha problem during the crosslinking process. The content of this work is the investigation of a complex material behavior of a structural adhesive BETAMATE™ 1480V203. The focus is on the determination of the behavior of the adhesive based on temperature. So, a bilinear temperature-dependent cohesive zone model pre-owned by the Institute für Füge- und Schweißtechnik is used in this work. The material behavior is validated with the help of FEM on geometrically simple structures such as Steel hat profile, Aluminium plate and mixed connections of both stated above and also on a glued multi-material BIW structure of a Toyota Camry model.

The goal is to increase the predictability of the stresses in the adhesive layer which happens during the drying process after CDC and also the relative displacements of the joining partners of bonded body-shell structures of the entire BIW. This is intended to lay foundations for providing a methodology for the multi-material BIW structures during hot curing of the paint drying process.

Prior to Chapter 2, a preface to the problems which arises during the paint drying process is reviewed in this chapter. In order to gain profound knowledge about this process, a comprehensive description is provided in the following unit.

## 2 State of the art

This unit covers the theme of the cathodic dip painting, adhesives in automobiles, the delta alpha problem and the associated strength of the adhesive bonds during the drying process after the CDC. Later in this chapter, the influence of thermal expansion behavior followed by the use of combination of different materials in current vehicle bodies is evaluated.

### 2.1 Cathodic dip painting

The electrophoretic deposition (EPD) is a widely used industrial process in which colloidal particles under the influence of an electric field are allowed to be deposited on an electrode. This is illustrated in the Figure 2.2a . Other name used for the electrophoretic deposition process is cathodic dip painting (CDP) [9].

Cathodic dip painting (also known as Kathodische Tauchlackierung) is an electrochemical process which ensures corrosion protection, quality, economy and environmental friendliness. This process is suited for series production and for painting of complex structures. It guarantees products which are resistant to salt water and stone chips. Durable products with high value retention are the result of this perfect surface sealing, which meets the high standards of car manufacturers. It also offers the best conditions for powder coating or conventional painting which makes the user independent in the choice of color and surface structure. The cathodic dip painting of a typical vehicle body is represented in Figure 2.1 .



Figure 2.1: Cathodic dip painting of a vehicle body [1]

Cathodic dip painting uses electrochemical process to separate paint. The physical principle underlying electrodeposition is that materials with opposite charges attract each other and thus achieve a very good adhesion. During the coating process, a

DC voltage is applied to the workpiece, which is then immersed in a paint bath with opposing paint particles. The paint particles are attracted to the workpiece, deposits and forms a uniform paint film over entire surface and it is shown in Figure 2.2b . Due to the electronic attraction, the paint adheres extremely strong to the metal and can penetrate corners and edges during the diving process. This process is continued until the coating has reached the specified layer thickness. With an appropriate layer thickness, the paint film has an insulating effect on the workpiece, thereby preventing electrical attraction and ending the coating process [10].

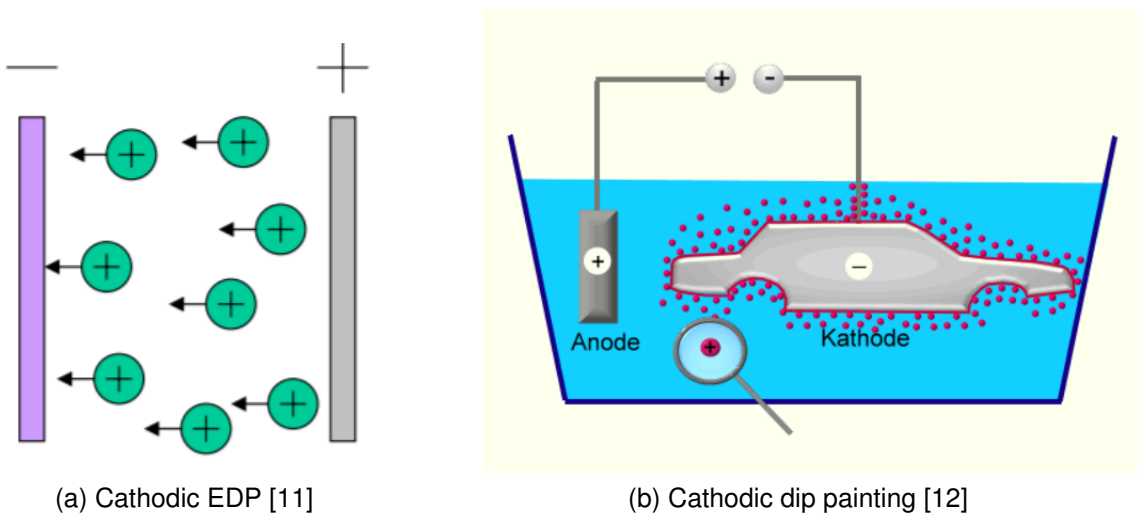


Figure 2.2: Schematic representation of cathodic dip painting process

Once the coating is finished, the whole body is then baked at 185 °C approximately to get a uniform surface thickness which ranges in the order of several micrometers. This is done after the coating process in order to ensure that, linear chain molecules are formed in the epoxy resin containing lacquer together with the blocked isocyanate, which are crosslinked three-dimensionally and thereby forming a stable structure. The crosslinking process usually takes place at higher temperatures [9]. A model of the paint drying oven which is used in many automotive companies is displayed in Figure 2.3 .

## 2.2 Adhesives in vehicle body construction

Due to the wide variety of materials which can be used in the construction of vehicle bodies, adhesive technology is currently experiencing boom in automotive industries for the past few years. This is due to the fact that modern lightweight materials and their combinations are preferred where for existing ones the joining procedures are difficult or not possible at all. The advantages of adhesive technology are different materials can be joined together, reduces the post-processing efforts, prevents con-



Figure 2.3: Paint drying oven [2]

tact corrosion, tension between the components can be balanced. Eventhough it has many advantages, it has some limitations such as connection strength which can only be achieved after curing process [13].

The adhesives in the body of a passenger car can be divided into groups based upon the functional point of view [3]. Adhesives in the supporting structures to connect load-bearing components often in combination with spot welds, to connect the stiffening profiles on the front or rear parts, flanged seam gluing for connecting thin sheets to doors and flaps and adhesive bonds for the force-transmitting connection of the washers with the vehicle structure. The scope of adhesive in modern body in white structures is exhibited in Figure 2.4 .

## 2.3 Delta Alpha problem during the paint-dryer process

In the case of mixed BIW construction, materials of different type are joined together. In practice, the effects caused by this are referred to as Delta Alpha problems. Different thermal expansions occur under isothermal conditions due to the different thermal expansion coefficients. The delta alpha problem describes the relative displacements in combination with the thermosetting adhesives and also the resulting

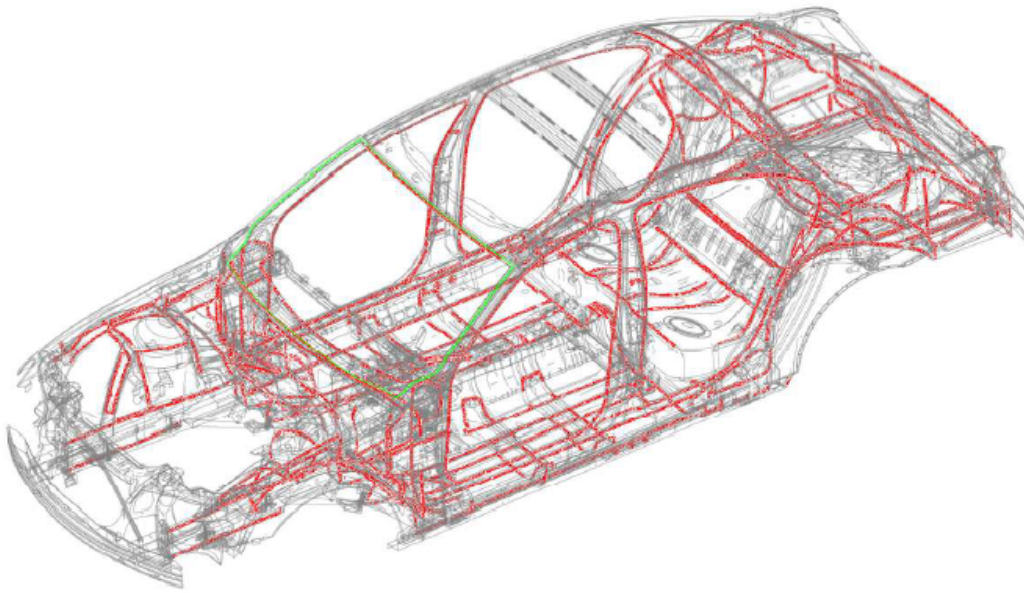


Figure 2.4: Scope of adhesive in modern BIW [3]

mechanical stress on the bonded joint and the joining partners. The coefficient of thermal expansion defines the change in length of a material in relation to the initial length due to a change in temperature [14]. In this work, the problems arised due to the mixed construction of using Steel and Aluminium parts is discussed. The thermal expansion coefficients of Steel and Aluminium is compared in Table 2.1 .

Table 2.1: Thermal expansion coefficients of Steel and Aluminium

Property	Symbol	Unit	Aluminium	Steel
Thermal expansion coefficient	$\alpha$	$K^{-1}$	$2.4e^{-5}$	$1.3e^{-5}$

The table shows that Aluminium expands more than Steel. In addition to this, epoxy resin adhesives which are often used to connect Steel and Aluminium have a lower thermal conductivity of about  $\leq 0.3 \text{ W m}^{-1}\text{K}^{-1}$  and thus also have an insulating effect [15]. This can further increase the difference in thermal expansion of Steel and Aluminium. However thermal deformations are not only limited to different thermal expansion coefficients, but can also rise from uneven temperature distribution in the component. As a result of inhomogenous heating of the joining partners, relative displacements occur and cause adhesive failure between the Aluminium and Steel parts.

If the adhesive surfaces of two joining partners are not firmly fixed during gluing, they

can move almost without force due to thermal expansion as long as the glue is in an uncrosslinked state. When there is an increase in temperature during the thermosetting, the adhesive behaves like a lubricant, since the viscosity initially decreases with increase in temperature. The part to be joined with larger thermal expansion coefficient slides relatively on the other part to be joined [7]. As a result of the adhesive crosslinking, the gliding still remains and generally leads to visible warpage of the parts to be joined and to stress relevant tensions in the adhesive layer.

The failure of adhesives in cooling phase is due to excessively high cooling rates and the resulting shifts in laboratory tests is the cause. According to [16], the following factors must be taken into account in the overall assessment of the factors influencing the strength of adhesive bonds that are exposed to sliding in the process:

- Elastic modulus of the materials of the joining part
- Relaxation in the adhesive
- Adhesive layer thickness
- Cross-section of the parts to be joined
- Adhesive surface
- Temperature differences of the parts to be joined
- Shear modulus of the connection in the curing process

In the successive section, the problems which are dealt with the adhesives during the paint dryer process is analyzed in short context. To identify the measures and to prevent the problems occurring in the adhesives, an idea about these is significant.



(a) Typical fracture surface [17]



(b) Adhesive crack [17]

Figure 2.5: Types of Adhesive damage

## 2.4 Adhesive problems during the paint-dryer process

During the drying process after cataphoretic dip coating, we tend to have some problems with the adhesives. These damages are the result of drying procedure after the cataphoretic dip coating process. Some types of the adhesive damages which occurs during this process are presented in Figures 2.5a and 2.5b .

In this Chapter 2, an insight into the CDP, adhesives in modern BIW and the delta-alpha problem is attained. In the consecutive Chapter 3, the approach for identifying problems should be determined. Accordingly, a plan is outlined for the same and elucidated.

# 3 Workflow of the simulation of cooling process

This chapter deals with the simulation workflow of the cooling process after the cataphoretic dip coating. In the following section a concise demonstration about the changes done in preprocessor ANSA™ is made. In the ensuing section an introduction to the FEM software ABAQUS™ is given and comes next the transient heat transfer and mechanical analysis explanation. The process workflow is illustrated in the Figure 3.1 .

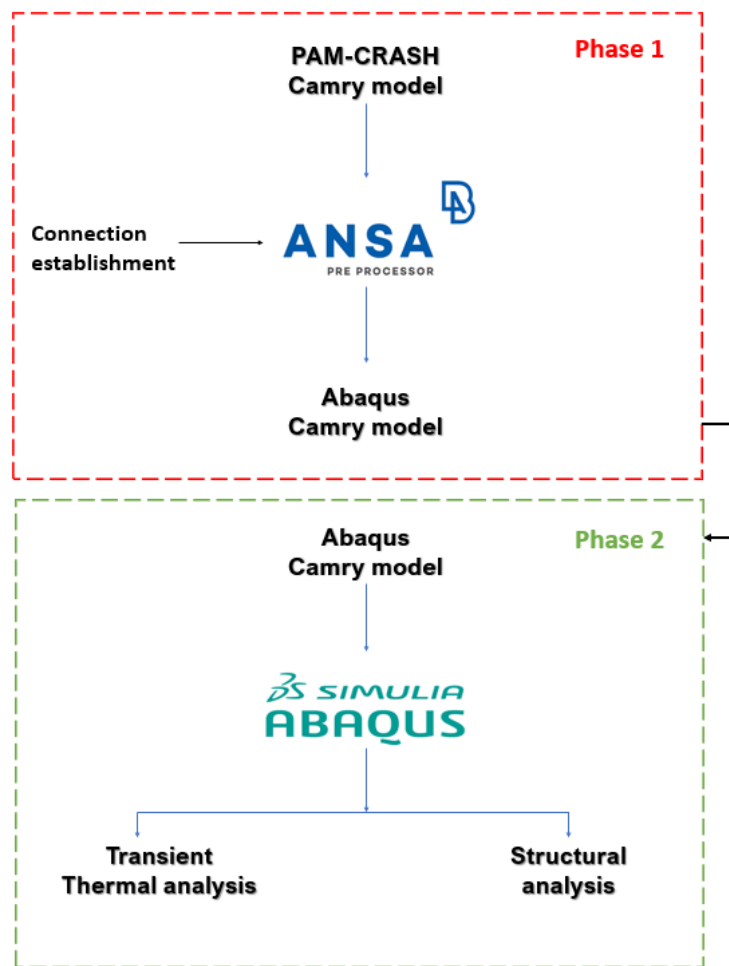


Figure 3.1: Phases in the simulation of cooling process

**Phase 1:** A model of Toyota Camry which is already available at GNS mbH is modified using the preprocessor ANSA™. The model is from a PAM-CRASH™ version which is to be converted into a readily available FEM model for simulation in ABAQUS™.

**Phase 2:** The converted model from PAM-CRASH™ has to be simulated in two steps in ABAQUS™.

**Step 1:** Initially, a transient heat transfer analysis is carried out to get the temperature results. The recommended thermal boundary conditions are added in this step.

**Step 2:** The resulting temperatures acts as a thermal load for the successive structural analysis of the Camry model.

### 3.1 ANSA™ preprocessor

ANSA™ is a CAE tool developed by the BETA CAE systems. It is a pre-processing tool that provides all the functionalities from designing phase to the ready-to-run solver input file in a single integrated environment [18]. In this project, the Toyota Camry model has to be modified from the PAM-CRASH™ database to the ABAQUS™ solver input file to carry out the analysis. ANSA™ v19.1.2 is used for this purpose.

The PAM-CRASH™ version Toyota Camry model which is shown in the below Figure 3.2 is imported into ANSA™. This model has to be reorganized into ABAQUS™ model using the connection manager features in ANSA™. The steps involved in the conversion is explained in the subsequent subsections.

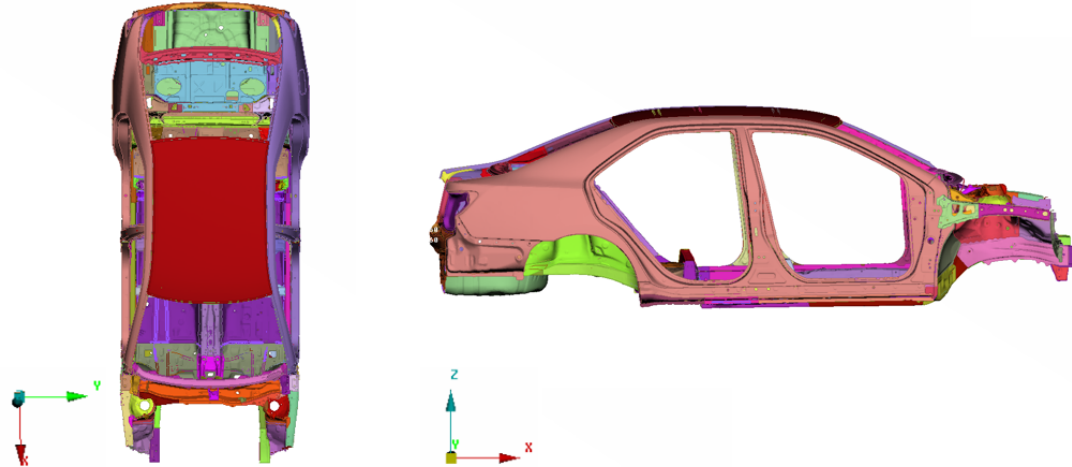


Figure 3.2: Top and side views of the Camry model

#### 3.1.1 Connection manager

Connection manager is one of the features available in the ANSA™ assembly option. This can be used for manipulating the connection entities present in the model. It can

### 3 Workflow of the simulation of cooling process

handle massive number of connection entities and acts as an interface for performing numerous actions [4]. Some of the actions are listed below:

- Connection entities can be "realized" (mesh-dependent or mesh-independent)
- FE-Representation of "realized" connection entities can be modified
- Connectivity informations can be viewed and modified
- The attributes of the connection entities such as width, height and diameter can be changed.

The connection manager window in ANSA<sup>TM</sup> is depicted in the Figure 3.3 which presents the basic information about the connotations present in it.

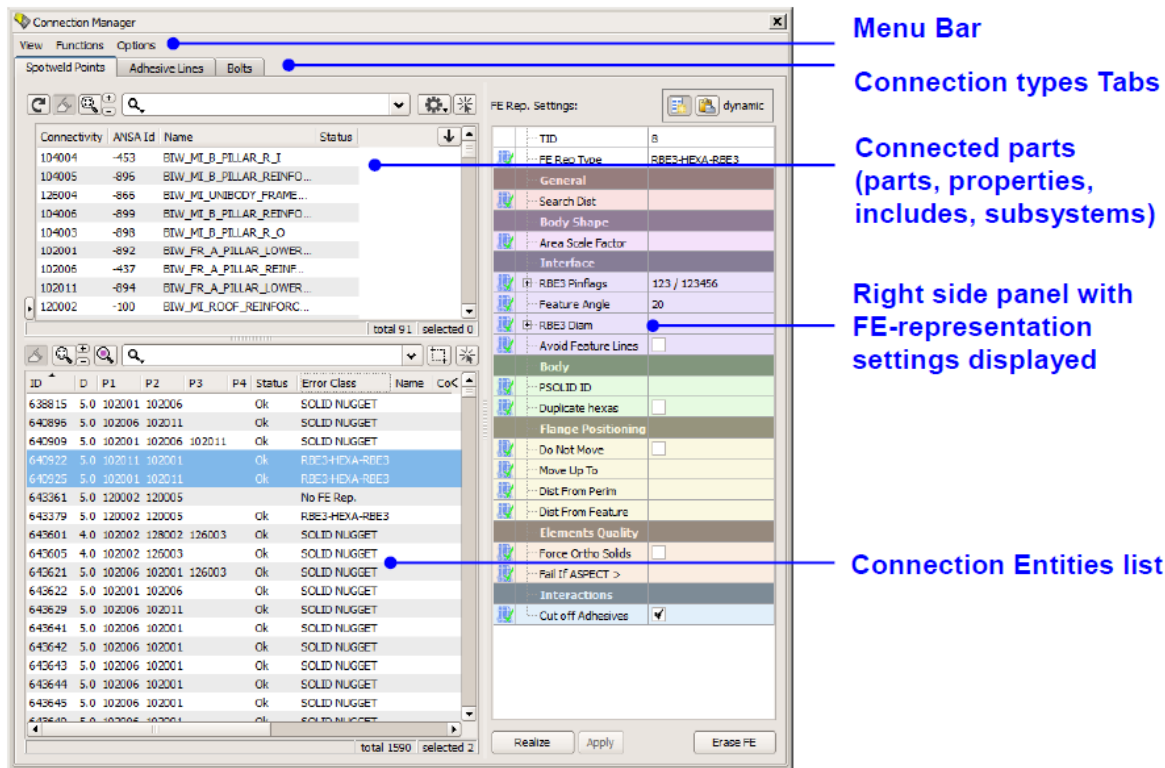


Figure 3.3: Connection manager tool in ANSA<sup>TM</sup> [4]

#### 3.1.2 Working with connection manager

Once the PAM-CRASH<sup>TM</sup> model is opened in ANSA<sup>TM</sup>, spot weld connections can be viewed in the left hand side of the application window as displayed in the Figure 3.4 . In this figure, there are lots of green circles present in the model. These are nothing but the PLINKS (FE representation of spot weld connections in PAM-CRASH<sup>TM</sup> database).

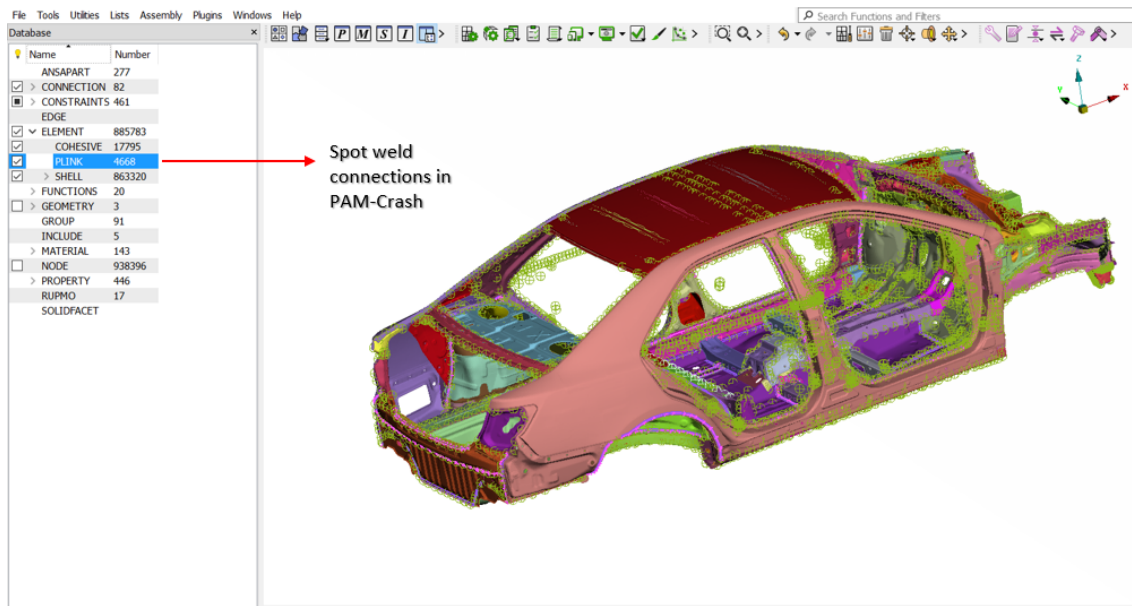


Figure 3.4: PLINKS in PAM-CRASH™ database

The first phase is converting these PLINKS to a suitable FE representation which can be modeled as spot weld elements in ABAQUS™. To convert the PLINKS, the FE representation has to be changed and it can be started as shown in the Figure 3.5 . After the selection of PLINKS, it has to be converted to FE connection points, so that it can be opened in connection manager and the desired changes can be done.

The next step is to convert the PLINKS to FE connection points. It must be made sure that the model is in PAM-CRASH™ solver deck module. Click the Assembly option in menu bar **Assembly** → **Convert** → **FE to Cnctn Pts** as presented in Figure 3.6 and select the whole area of PLINKS in the application window and press the middle mouse button. Now the PLINKS will be converted into FE connection points. Then switch to the ABAQUS™ solver deck module.

To open the connection manager, there are two ways. The first is by clicking the **Assembly** → **Connection manager** or by clicking in the assembly buttons. Once after doing that, select the **Visible Ents** in the search entry of the connection selection assistant dialog box. After selecting it, press the **Show** button and select all the FE connection points available in the application window. Then press the middle mouse button or the scroll button, so that the attributes or the FE representation type can be changed via the connection manager.

After the connection manager dialog box is opened as illustrated in the Figure 3.7, the user can change the diameter of the spot welds and the FE representation of the spotweld which can be implemented in ABAQUS™.

### 3 Workflow of the simulation of cooling process

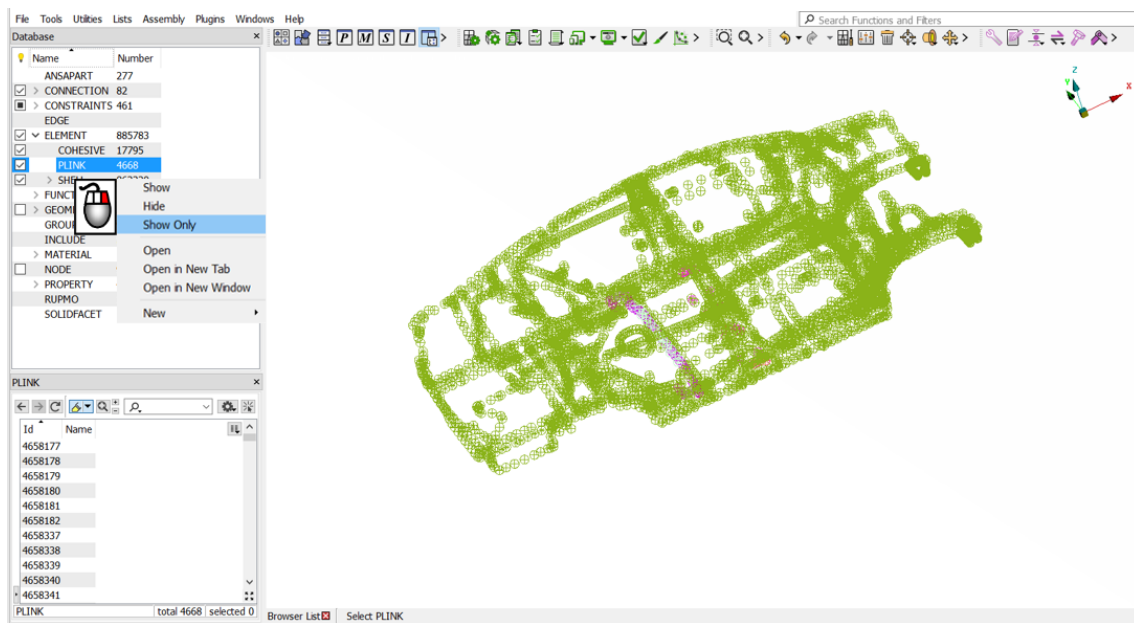


Figure 3.5: Selection of PLINKS

The process of converting the PLINKs from PAM-CRASH™ solver deck module to desired FE representation type in ABAQUS™ solver deck module is exhibited in schematic flow diagram (see Figure 3.8).

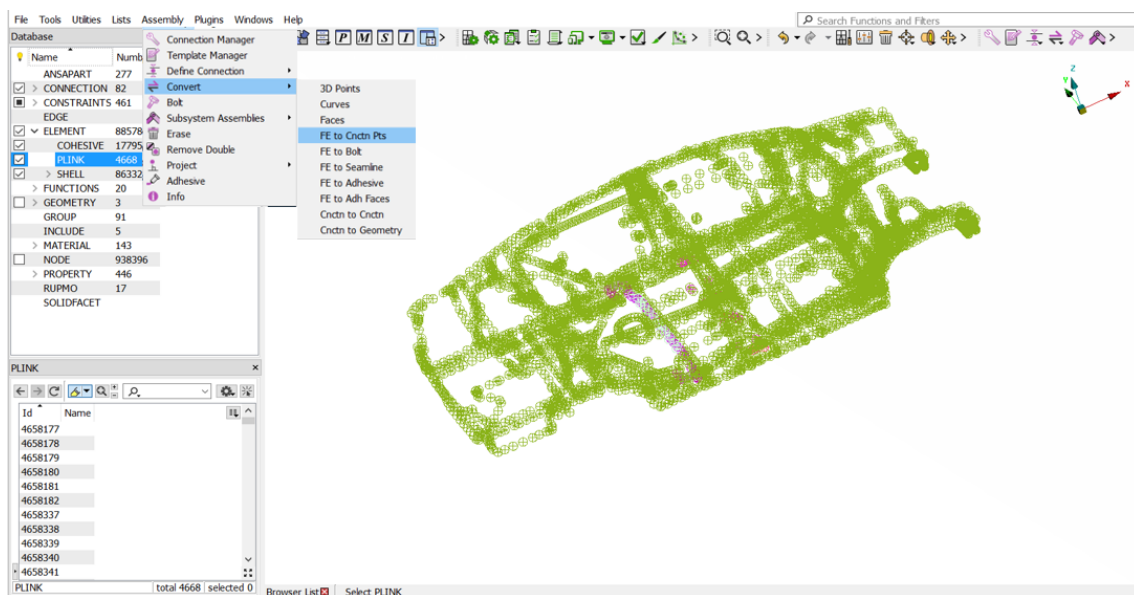


Figure 3.6: Conversion of PLINKS to connection points

In this project, the desired type of FE representation in ABAQUS™ is chosen as DYNA spotweld. This is chosen because it is connected to the parts via \*TIED contact. This in turn is very much helpful for simulating the heat transfer through spotwelds in transient heat transfer analysis in ABAQUS™.

### 3 Workflow of the simulation of cooling process

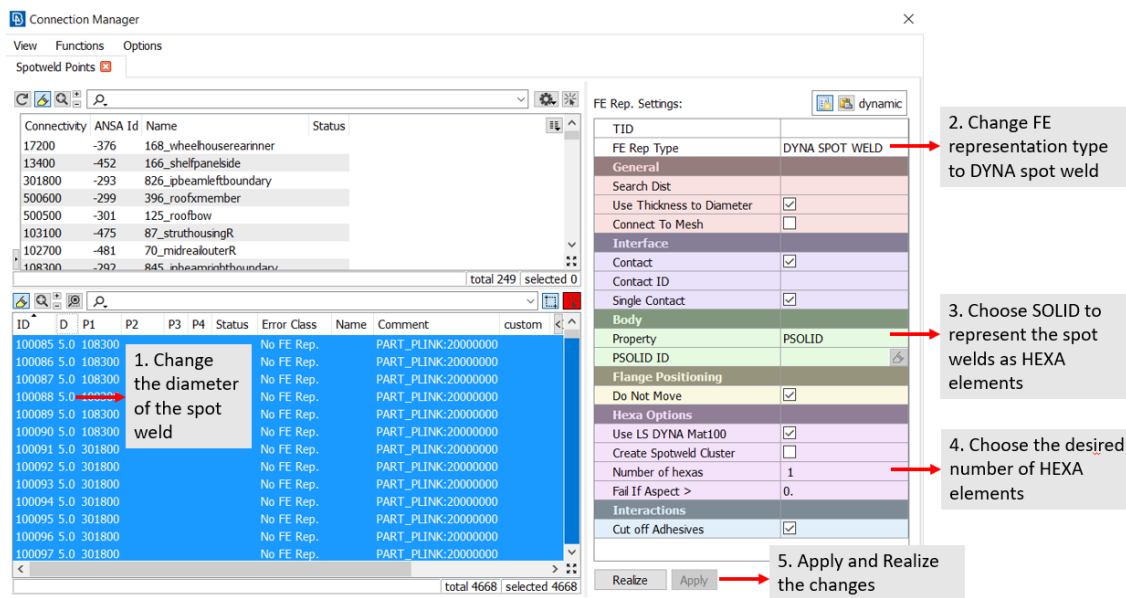


Figure 3.7: Change to suitable FE representation type in connection manager

The DYNA spotwelds are chosen as SOLID property so that they are connected to the parts by HEXA elements. In some places where the connections fails to realize, they can be realized by increasing the number of HEXA elements. After the successful completion of this process, the PLINKS will be converted into DYNA spotwelds which can be used as heat transfer elements as well as stress elements in ABAQUS™ solver.

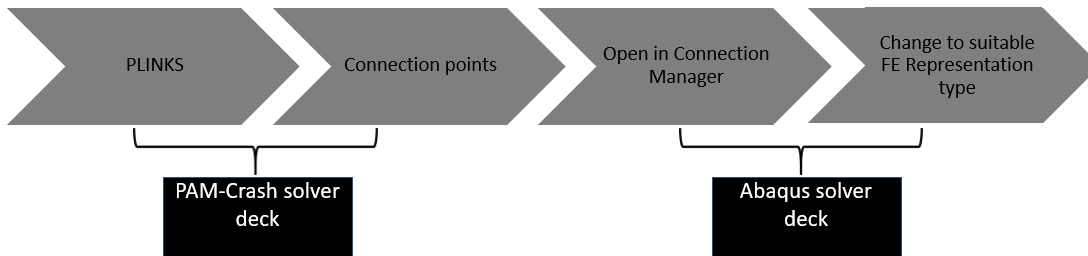


Figure 3.8: Conversion of PLINKS to suitable FE representation type in ABAQUS™

#### 3.1.3 Surface set definition for Steel and Aluminium

Normally, if a film condition is defined for the solid element model it will be applied on all surfaces of the model. This is not the case when it comes to shell element FE model. It must be ensured that the film condition is applied on all surfaces of the shell element model to get a proper cooling condition from the initial temperature to the room temperature. This is the next and final step in ANSA™ preprocessor.

The temperature-dependent film condition should be defined on the top and bottom surfaces of the shell element model. This can be achieved by creating a separate surface sets for Steel and Aluminium parts. Create a new set by right clicking **SET** → **NEW** → **NEW**. Choose the **PROPERTY** → **SHELL\_SECTION** and the corresponding parts for which the surface sets has to be assigned. For example, if a surface set has to be created for the Aluminium parts, choose only the Aluminium parts from the **SHELL\_SECTION** and create the surface sets for them.

After selecting the parts from the **SHELL\_SECTION**, a dialog box will be opened for creating the SET as shown in Figure 3.9 . In the dialog box, the **Output as** option should be selected as SURFACE and the orientation can be selected as SPOS or SNEG. The same procedure can be repeated to create the surface sets for Steel parts.

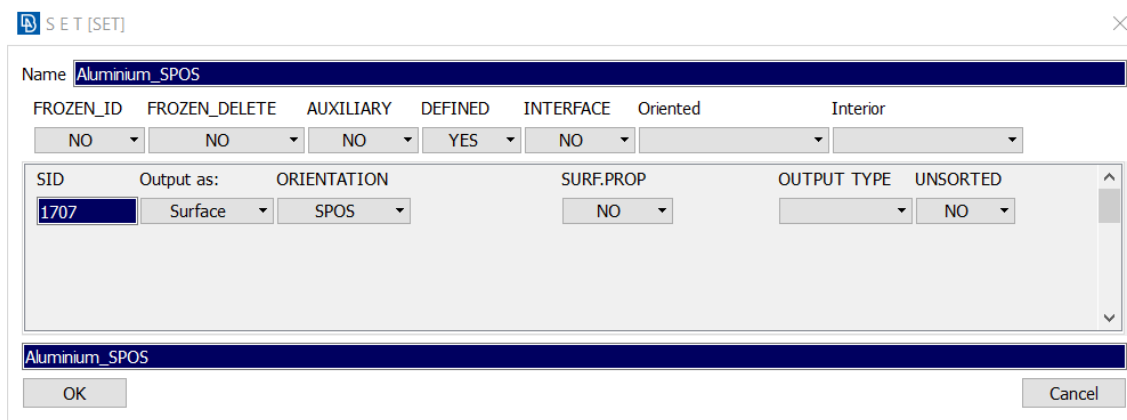


Figure 3.9: Surface set creation for Aluminium part

This step of creating the surface sets has to mandatorily done in ANSA<sup>TM</sup> because for a complex model it is difficult to define the surface sets in ABAQUS<sup>TM</sup>.

In the next section, the basic idea of simulating the transient thermal analysis and mechanical analysis in ABAQUS<sup>TM</sup> is deliberated.

## 3.2 ABAQUS<sup>TM</sup> FE solver

ABAQUS<sup>TM</sup> is a CAE tool and FEA solver developed by Dassault systemes<sup>®</sup> in 1978. It consists of five core software products. In this project, two software products are used and discussed [19].

**Abaqus<sup>TM/CAE</sup>**: It supports the users to create geometry, import CAD models for meshing or integrate geometry based meshes. The interface is very much interac-

tive so that the users can customize the GUI options [20].

**Abaqus™/Standard:** It is a general purpose finite element analyzer. As traditional FEA solvers, Abaqus™/Standard employs implicit integration scheme [19].

ABAQUS™ 2016 is used in this work to perform the simulations.

### 3.2.1 Thermo-Mechanical analysis

In Thermo-Mechanical problems, there are two fields that has to be determined. On application of thermal load the materials expand. This means that the two fields temperature and displacement are linked with each other. So, this is kind of a coupled problem. This kind of coupled problem can be solved in ABAQUS™ by solving the thermal problem first and then the mechanical problem. This is known as sequentially coupled thermal-stress analysis in ABAQUS™. The following subsection describes the way of solving the problem.

### 3.2.2 Sequentially coupled thermal-stress analysis

A sequentially coupled thermal-stress problem is used where a displacement or stress fields are depending upon the temperatures. This is performed by conducting an uncoupled heat transfer analysis and then a displacement/stress analysis. In this the temperature does not depend on the stress analysis and a common example of sequential multiphysics workflow [21]. A brief description is given to each of the module in ABAQUS™.

#### • Part

The part from the ANSA™ preprocessor is imported into ABAQUS™ as an input(.inp) file. This file has the data of the nodal coordinates and properties (if any defined in ANSA™) and so on.

#### • Property

The property definition will be separate for the thermal and mechanical analysis. Initially for the thermal analysis properties such as Density, Specific heat capacity and Thermal conductivity are defined. Mechanical properties such as elasticity parameters, coefficient of Thermal expansion and plasticity properties must be defined for the mechanical analysis. The section assignment for the cohesive elements during the thermal analysis must be assigned properly. The thickness for the cohesive element should be specified during the mechanical analysis as it plays an important role in detecting the mechanical stresses in the adhesive.

### • Step

In the Step module, both the heat transfer and mechanical analysis will be run for 2400 seconds in order to simulate the cooling process from 180 °C to room temperature.

### • Interaction

In the thermal analysis, since a cooling process is simulated, the convective heat transfer comes into picture. Hence, temperature-dependent film coefficients are ascertained by experiments and validated in ABAQUS™ (see Chapter 4) to use the same for the Toyota Camry model.

### • Load

An initial condition is defined with predefined temperature field as a load condition. The nodal temperatures are obtained as results from this. These temperature results are defined as the loading condition for the successive mechanical analysis.

### • Mesh

The Abaqus™/Standard offers shell heat transfer elements such as DS4,DS3 and solid heat transfer elements DC3D8 which are used for the parts and spotwelds respectively. For example, if a DS4 element defined by nodes 100,101,102,103 is used in the thermal analysis, corresponding three dimensional shell element type S4R should be used in the stress analysis procedure [21].

### • Output

The nodal temperatures (NT) are requested as output by requesting the output variable from the thermal analysis. This is read into the mechanical analysis as a pre-defined field. The output variables such as von Mises stress (S), Total strain components (E), Plastic strain components (PE), Displacements (U), Scalar stiffness degradation (SDEG), Damage Initiation criteria (DMICRT) and Status variables (STATUS) are requested from the mechanical simulation.

The present and the preceding chapters dealt with the strategy for the simulation and information about the procedure such as drying process of CDP and so forth. Since the idea for establishing the steps discussed previously is constructed, in the next phase the validation of the material properties must be done to use it for the simulations. This is explained briefly in Chapter 4 .

# 4 Material model validation

This unit involves validation of properties for the thermal and mechanical analysis by using applicable models for Steel and Aluminium. The predominant point is about using the appropriate temperature based film coefficients for the materials, because the convective heat transfer depends upon this. In the subsequent sections, the temperature based film coefficients obtained based upon laboratory experiments and validating it using the FEM software ABAQUS™ is taken up.

## 4.1 Steel hatprofile

In this section, the validation of temperature based film coefficients which has to be used for the parts made up of Steel in Toyota Camry model is conferred. So, a laboratory experiment of cooling process is conducted and the Steel hatprofile is made to cool from 180 °C to room temperature. Then the temperatures are recorded using thermocouples as well as verified the temperature results with a Thermal imaging camera. The experimental setup which demonstrates the cooling process is presented in the Figure 4.1 . The experimental procedure for the Steel hatprofile is done

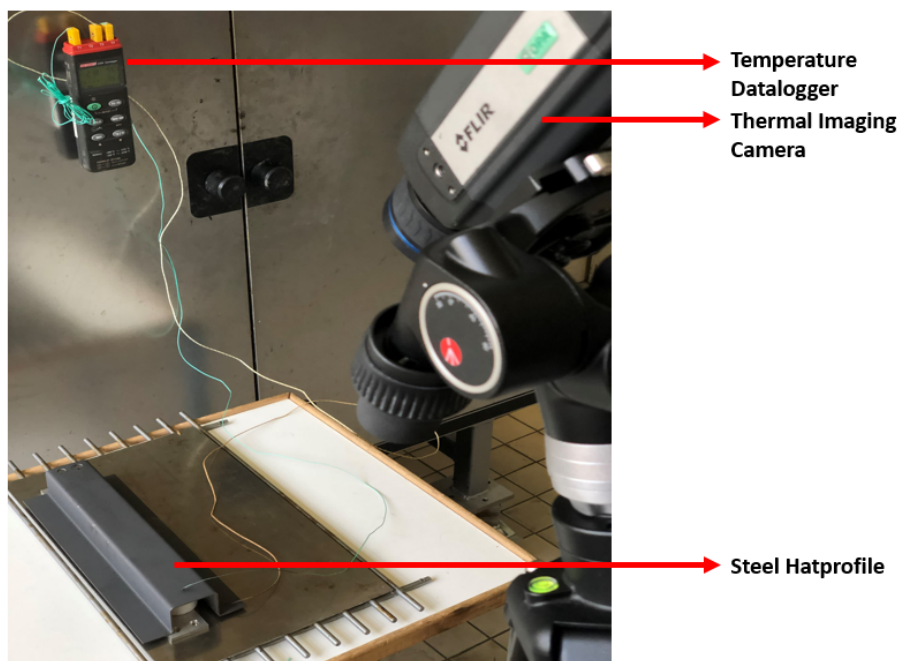


Figure 4.1: Experimental cooling process of DC01 Steel hatprofile

in the Institut für Füge- und Schweißtechnik laboratory at TU Braunschweig. The device arrangement and the method in which it is conducted is demonstrated in the subsection 4.1.1 .

### 4.1.1 Experimental procedure of Steel hatprofile

The experiment is conducted thrice on three different days to assure about obtaining the right choice of temperature-dependent film coefficients. In the Figure 4.2 shows a Steel hatprofile of grade DC01, length 300mm and thickness 2mm. Initially, the Steel hatprofile is heated in a oven until it reaches 180 ° C. Then the setup is taken outside and placed on the table to conduct the cooling process from 180 ° C to room temperature. The temperatures are measured at two different points using thermocouples and recorded with a temperature datalogger to know about the temperature distribution. The thermocouples are welded at those points so as to guarantee that it does not move while taking the setup out from the oven after heating. In addition to this, another thermocouple is used to record the room temperature and is attached to the datalogger. The Steel hatprofile is coated with a black paint to avoid unnecessary reflections from the surface while capturing with the TIC. An insulation material and support are used for preventing the hatprofile from coming into contact with the ground surface.

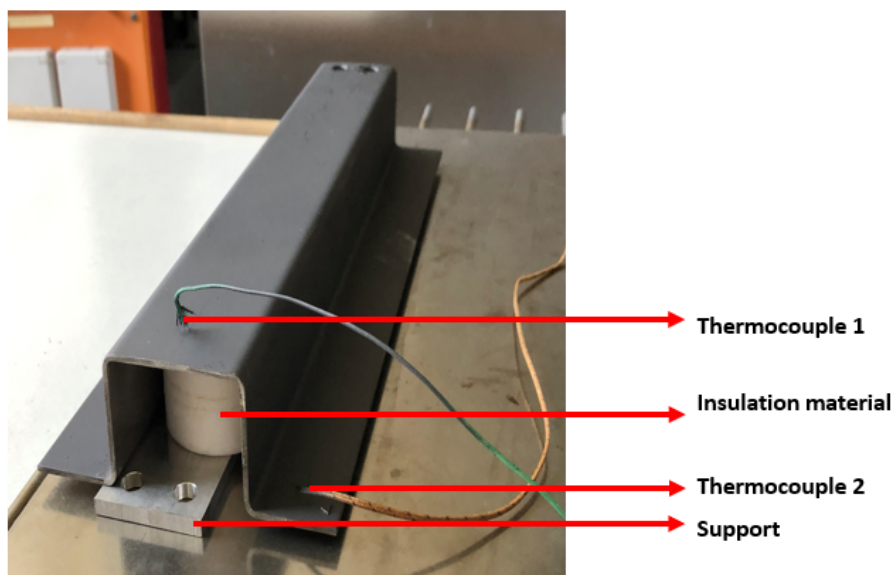


Figure 4.2: DC01 Steel hatprofile

sary reflections from the surface while capturing with the TIC. An insulation material and support are used for preventing the hatprofile from coming into contact with the ground surface.

Table 4.1: Different room temperatures of the conducted experiments

<b>Experiments</b>	<b>Room Temperature [°C]</b>
Experiment 1	23
Experiment 2	20.5
Experiment 3	18

This experimental process is repeated three times on three different days (with different room temperatures) to decide the finalized temperature-dependent film coefficients.

ficients. Table 4.1 provides the three different room temperatures during which the experiments were conducted. Figure 4.3 illustrates the cooling rate of the three experiments performed.

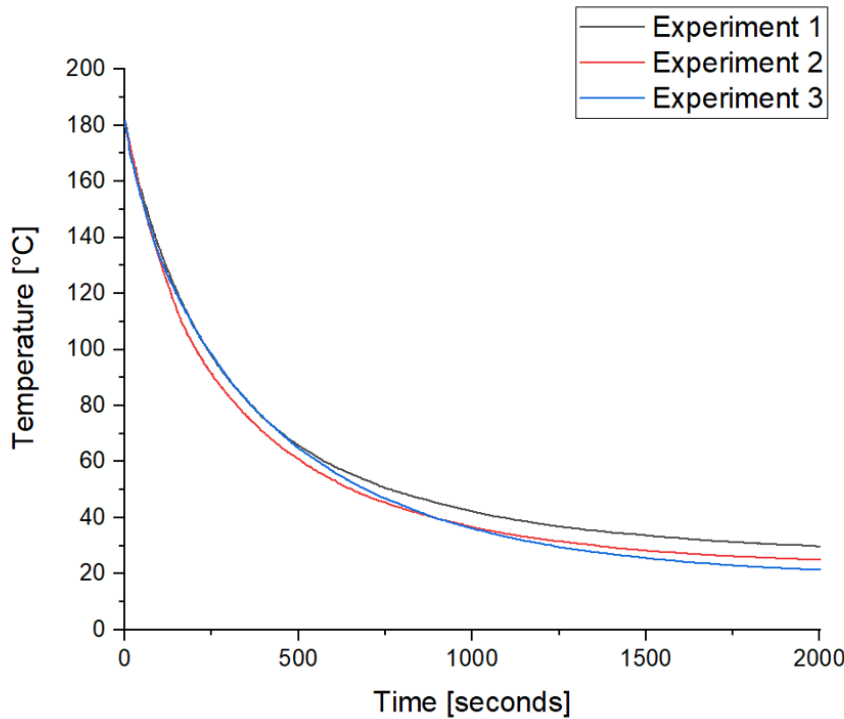


Figure 4.3: Experimental cooling rate of the DC01 Steel hatprofile

In the next step a FE model of same dimensions has to be modeled and confirm the affiliation with the temperature data obtained from the experiments.

#### 4.1.2 Simulation of Steel hatprofile

The simulation of the above explained experimental procedure is done in the Abaqus™/Standard and examined. A Steel hatprofile FE model which is displayed in the Figure 4.4 is modeled in ABAQUS™.

The properties such as Density, Specific heat and Thermal conductivity which are used for thermal analysis in ABAQUS™ are summarized in Table 4.2 . The simulation

Table 4.2: Thermal properties used for DC01 Steel

Property	Symbol	Unit	Steel
Density	$\rho$	ton mm <sup>-3</sup>	7.85e <sup>-9</sup>
Thermal conductivity	$k$	mW mm <sup>-1</sup> K <sup>-1</sup>	52
Specific heat capacity	$c$	mJ ton <sup>-1</sup> K <sup>-1</sup>	0.48e <sup>9</sup>

is done thrice so as to match the three experimental results and carried out for a

time period of 2400 seconds. An initial condition of  $180^{\circ}\text{C}$  is applied as thermal load for the simulation model and allowed it to cool down to room temperature. This procedure is based upon the temperature-dependent film coefficients which is used for three different simulations matching the experimental data. The elements used in the simulation are solid heat transfer elements DC3D8 (An 8-node linear heat transfer brick) since the Steel hatprofile modeled in Abaqus<sup>TM</sup>/CAE is of type solid.

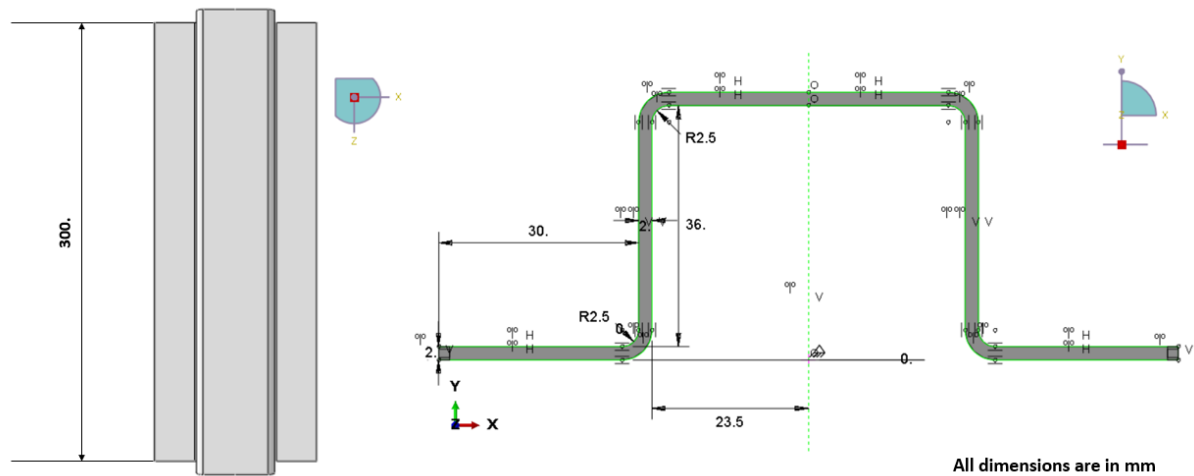


Figure 4.4: Dimensions of Steel hatprofile model in ABAQUS<sup>TM</sup>

The sink temperature or room temperatures for each of these simulations are based upon the three different experimental room temperatures as mentioned in Table 4.1 . The temperatures are measured at two points A and B in the simulation model same as the experimental model. Since the two points almost had the same temperatures throughout the process, simulation temperatures from point A is compared with the experimental data. The points at which the temperatures are measured is represented in the Figure 4.5 . The temperature dependent film coefficients obtained from the simulations are listed in the Table 4.3 .

Table 4.3: Temperature-dependent film coefficients obtained from ABAQUS<sup>TM</sup>

<b>Simulation 1 film coefficient [mW mm<sup>-2</sup>K<sup>-1</sup>]</b>	<b>Simulation 2 film coefficient [mW mm<sup>-2</sup>K<sup>-1</sup>]</b>	<b>Simulation 3 film coefficient [mW mm<sup>-2</sup>K<sup>-1</sup>]</b>	<b>Temperature [°C]</b>
0.003	0.005	0.006	20
0.008	0.009	0.008	80
0.012	0.012	0.012	140

The room temperature or sink temperature used for Simulation 1 is  $23^{\circ}\text{C}$ , Simulation 2 is  $20.5^{\circ}\text{C}$  and Simulation 3 is  $18^{\circ}\text{C}$  respectively in correspondence with experimental room temperatures. The film coefficients for each of these simulations vary because, the room temperature varies in each of the experiments and tends to have

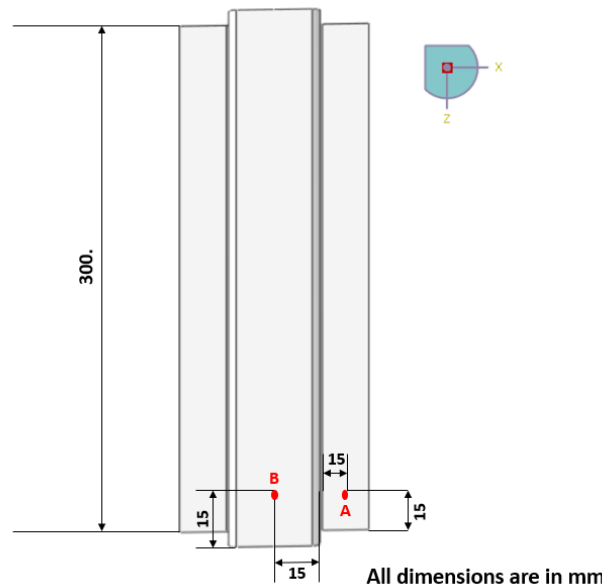


Figure 4.5: Temperature measurement points in ABAQUS™ for DC01 Steel

a slower cooling rate with one another. The temperature data obtained from the simulations at point A is plotted against the experimental temperature data to ensure a proper fit. The graphical fits for the Simulation 1, Simulation 2 and Simulation 3 are presented in Figures 4.6 - 4.8 . The temperature-dependent film coefficients for the Steel material is finalized by interpolating the values from the simulations based on temperatures 20 °C, 80 °C, 140 °C respectively. The decided values for the Steel

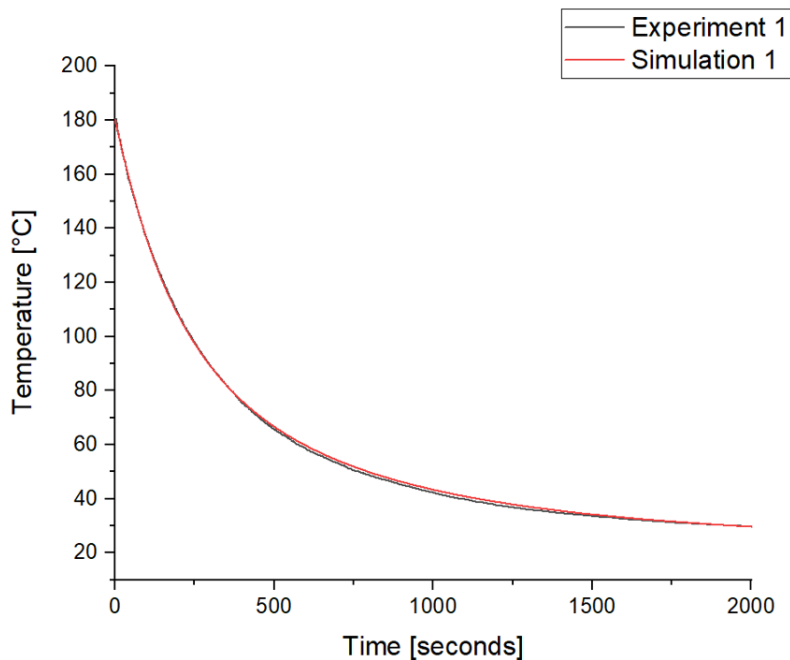


Figure 4.6: Experiment 1 cooling rate vs Simulation 1 cooling rate for DC01 Steel

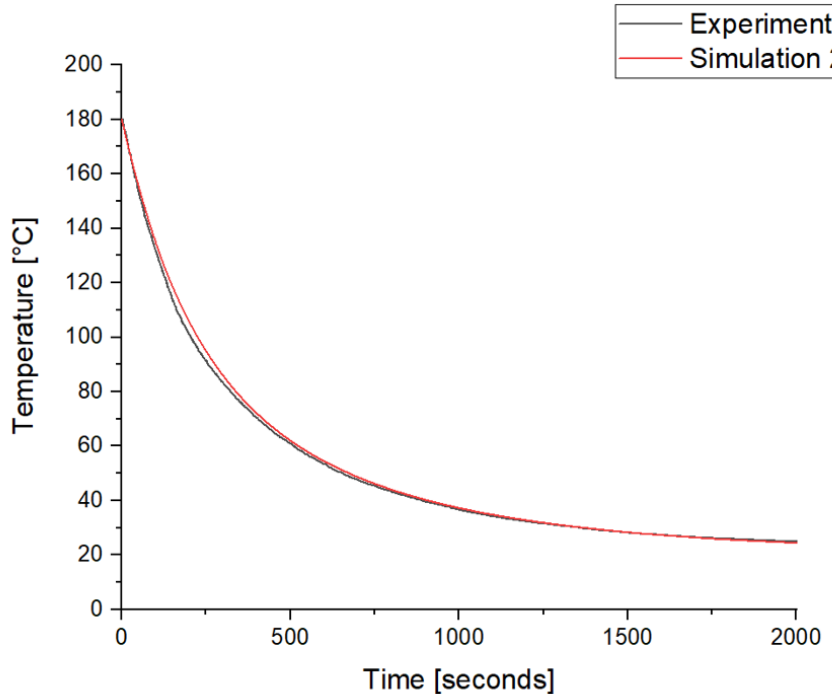


Figure 4.7: Experiment 2 cooling rate vs Simulation 2 cooling rate for DC01 Steel

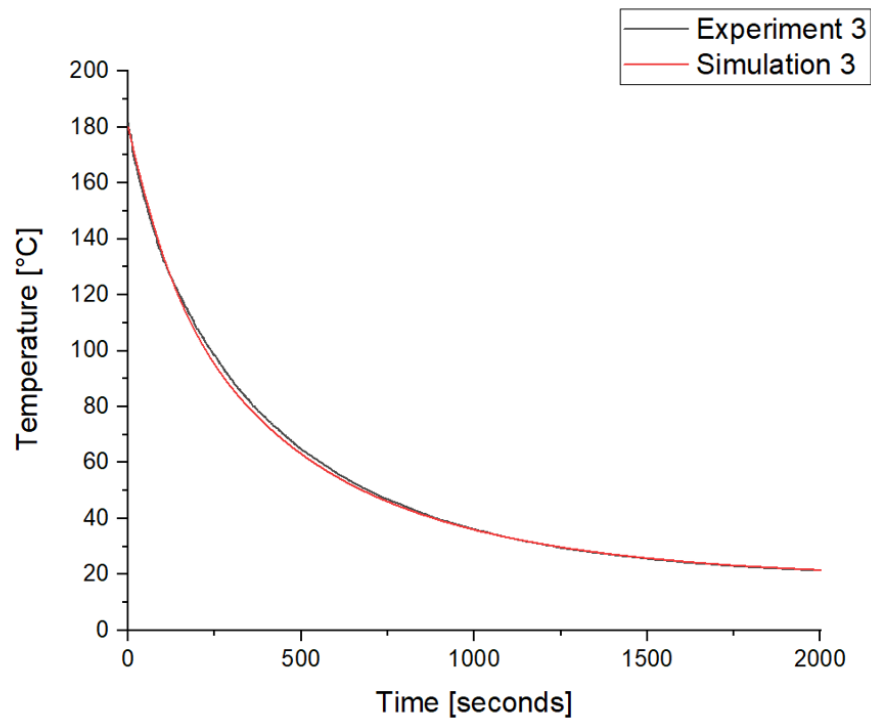


Figure 4.8: Experiment 3 cooling rate vs Simulation 3 cooling rate for DC01 Steel

material are exhibited in the Table 4.4 . This set of values is agreed to use as the film coefficients in the thermal analysis of the Toyota Camry model.

Table 4.4: Temperature-dependent film coefficients finalized for Steel material

Finalized simulation film coefficient [mW mm <sup>-2</sup> K <sup>-1</sup> ]	Temperature [°C]
0.004	20
0.008	80
0.012	140

The material model validation for Aluminium of grade EN AW-6082-T6 is conferred in the next section with the same kind of experimental procedure conducted for Steel hatprofile.

## 4.2 Aluminium plate

In this section, the validation of temperature-dependent film coefficients which is to be used for the parts made up of Aluminium is verified. So, same as like that of a laboratory experiment of cooling process done for the Steel hatprofile (see Section 4.1.1) another experiment is conducted for the Aluminium plate. The temperatures are recorded using the temperature datalogger.

### 4.2.1 Experimental procedure of Aluminium plate

The experiment is conducted once to decide about the temperature dependent film coefficients. Since only two parts are made up of Aluminium in the whole Toyota Camry model and the experiment is in good correlation with the simulation results, the further experiments has not been done. The experimental procedure for the Aluminium plate is done in the Institut für Füge- und Schweißtechnik laboratory at TU Braunschweig.

An Aluminium plate of grade EN AW-6082-T6, length 320mm and thickness 5mm is used for the experiment. Initially, the Aluminium plate is heated in the oven until it reaches 180 ° C. Then it is taken outside and allowed to cool from 180 ° C to room temperature. The temperatures are measured at two different points using thermocouples and recorded with a temperature datalogger to know about the temperature distribution. Another thermocouple is used to measure the room temperature and attached to the datalogger. The cooling rate for the experimental procedure of Aluminium grade EN AW-6082-T6 is shown in the Figure 4.9 .

In the next step a simulation model of same dimension of the Aluminium plate has to be modeled in Abaqus™/CAE and validate the temperature data obtained from the experiment.

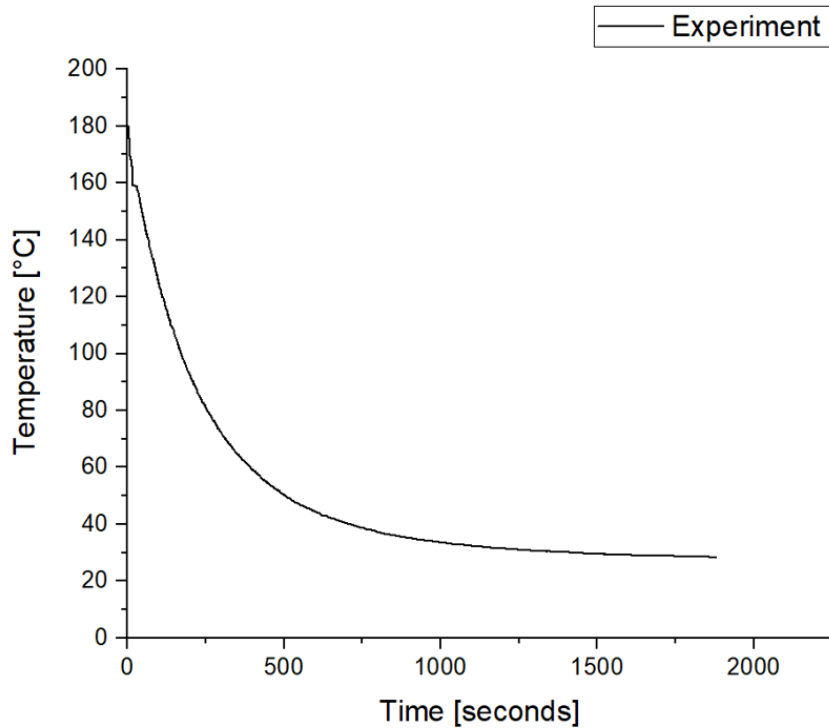


Figure 4.9: Experimental cooling rate of the EN AW-6082-T6 Aluminium plate

#### 4.2.2 Simulation of Aluminium plate

The simulation for EN AW-6082-T6 Aluminium plate is done in the same procedure as like that of the Steel hatprofile (see Section 4.1.2). An Aluminium plate FE model which is presented in Figure 4.10 is modeled using Abaqus<sup>TM</sup>/CAE.

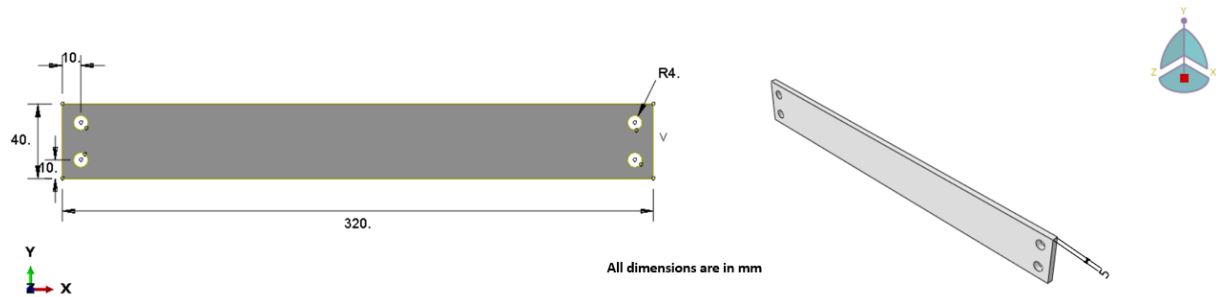


Figure 4.10: Dimensions of Aluminium plate model in ABAQUS<sup>TM</sup>

Table 4.5 lists the properties such as Density, Thermal conductivity and Specific heat capacity which are used for thermal analysis of Aluminium plate in ABAQUS<sup>TM</sup>. The simulation is carried out for a time period of 1950 seconds. An initial condition of 180 °C is applied as a thermal load for the simulation and allowed it to cool down to room temperature 26 °C based upon the temperature-dependent film coefficients which is used to match the experimental data. The elements used in the simulation

Table 4.5: Thermal properties used for EN AW-6082-T6 Aluminium

Property	Symbol	Unit	Aluminium
Density	$\rho$	ton mm <sup>-3</sup>	2.71e <sup>-9</sup>
Thermal conductivity	$k$	mW mm <sup>-1</sup> K <sup>-1</sup>	237
Specific heat capacity	$c$	mJ ton <sup>-1</sup> K <sup>-1</sup>	0.91e <sup>9</sup>

are solid heat transfer elements DC3D8 (An 8-node linear heat transfer brick), since the Aluminium plate modeled in Abaqus™/CAE is of type solid.

The temperatures are measured at two points A and B in the simulation model same like the experimental model. Since the two points chosen are symmetric to the model, the temperatures for both points A and B are the same. So, the simulation temperature data from point A is compared with the experimental data. The points at which the temperatures are measured is depicted in Figure 4.11 . The temperature-dependent film coefficients obtained from the simulation is shown in the Table 4.6 .

Table 4.6: Temperature dependent film coefficients obtained from ABAQUS™

Finalized simulation film coefficient [mW mm <sup>-2</sup> K <sup>-1</sup> ]	Temperature [°C]
0.008	20
0.023	80



Figure 4.11: Temperature measurement points in ABAQUS™ for EN AW-6082 Aluminium

The room temperature or sink temperature used for Simulation 1 is 26° C. The temperature data obtained from the simulation at point A is plotted against the experimental temperature data to ensure a proper fit. This is shown in Figure 4.12 .

So, the temperature dependent film coefficient for Aluminium is finalized and can be used for the parts made up of Aluminium in Toyota camry model.

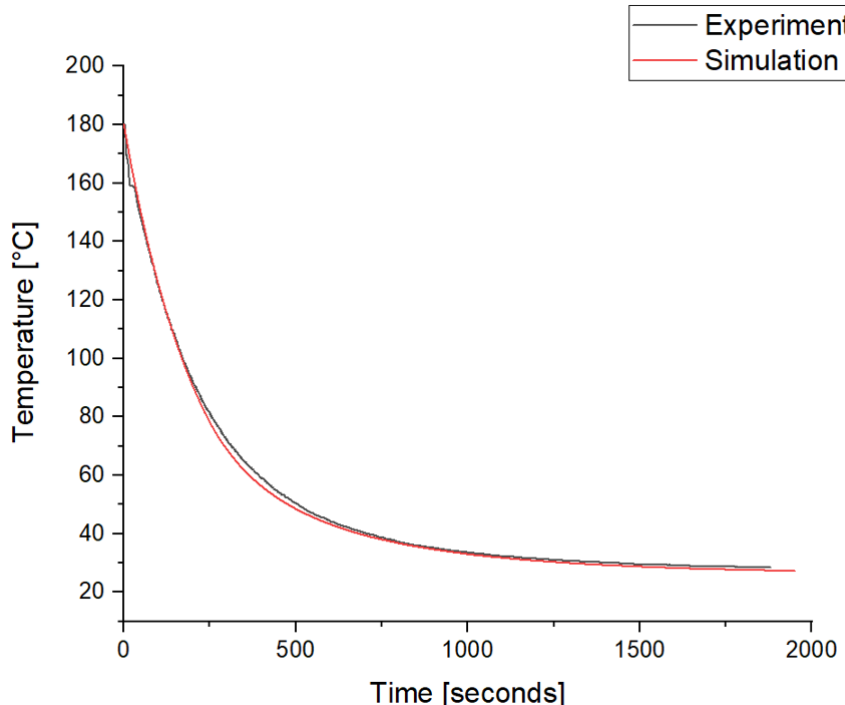


Figure 4.12: Experiment 1 cooling rate vs Simulation 1 cooling rate for EN AW-6082-T6 Aluminium

The consecutive section describes a simple prototype where both Aluminium and Steel parts are made of shell elements which is used for thermal and mechanical analysis and drives the way for decisive simulation method for Camry model.

## 4.3 Combined Steel and Aluminium profiles with shell elements

In the earlier sections thermal analysis is done for simple solid models to obtain the film coefficients. Now a procedure should be finalized for the simple prototype made of shell elements so that, it can be applied in the vehicle model as the parts are made up of shell elements.

### 4.3.1 Combined shell model description

A model is created in ANSA™ preprocessor with the same dimensions as that of the Steel Hatprofile (see Figure 4.4) and Aluminium plate (see Figure 4.10) reviewed in the preceding sections. There is a slight change in the model (not dimensions), where the holes in the Aluminium plate are closed and replaced by two spot weld elements. Then a ABAQUS™ model (.inp) file is generated using the ABAQUS™ solver deck module in ANSA™. It is then imported into Abaqus™/CAE and is illustrated in

Figure 4.13, where the Steel profile and Aluminium plate are fixed with adhesive at one end and spotwelds on the other end. Practically, though the Aluminium and Steel cannot be welded together, for simulation robustness it is assumed to be welded. Both Steel and Aluminium parts are made up of shell elements. The enlarged views



Figure 4.13: A view of combined shell model

of the spotwelds and adhesive where the Steel and Aluminium plate are fixed to one another is presented in Figure 4.14 .

A description about the adhesive used is made clear in the immediate section and the ensuing sections illustrates the thermal analysis and resulting mechanical analysis of the combined shell model.

### 4.3.2 Description of the adhesive used

The adhesive used in this combined shell model as well as for the investigation of Toyota Camry model is a one component heat curing epoxy-based adhesive manufactured by Dow Automotive GmbH , Dillenburg, Germany referred to as BETAMATE™ 1480V203. This will be used to predict the adhesive failure during manufacturing processes using a bilinear temperature-dependent cohesive zone model in ABAQUS™ [8]. The structural adhesive is manufactured for the use in body shop. It has very good adhesion properties on pretreated aluminium, automotive steels and coated steels. This type of adhesive is generally used to increase crash performance, body stiffness and operational durability [22]. Furthermore, the adhesive is in non-crosslinked state during the process of cataphoretic dip coating(CDC). The crosslinking takes place in the drying oven of the CDC process [7] .

The thermal properties for the adhesive is finalized based on the research project [23] and the technical datasheet of BETAMATE™ 1480V203 [22]. The mechanical properties of the adhesive is finalized based on the temperature-dependent cohesive zone model developed by Institut für Füge- und Schweißtechnik, TU Braunschweig which can be used to predict the damage during drying process [8]. The thermal properties used for the adhesive is listed in the Table 4.7 . Since the CZM is developed using the approach of bilinear traction seperation, the model assumes a linear

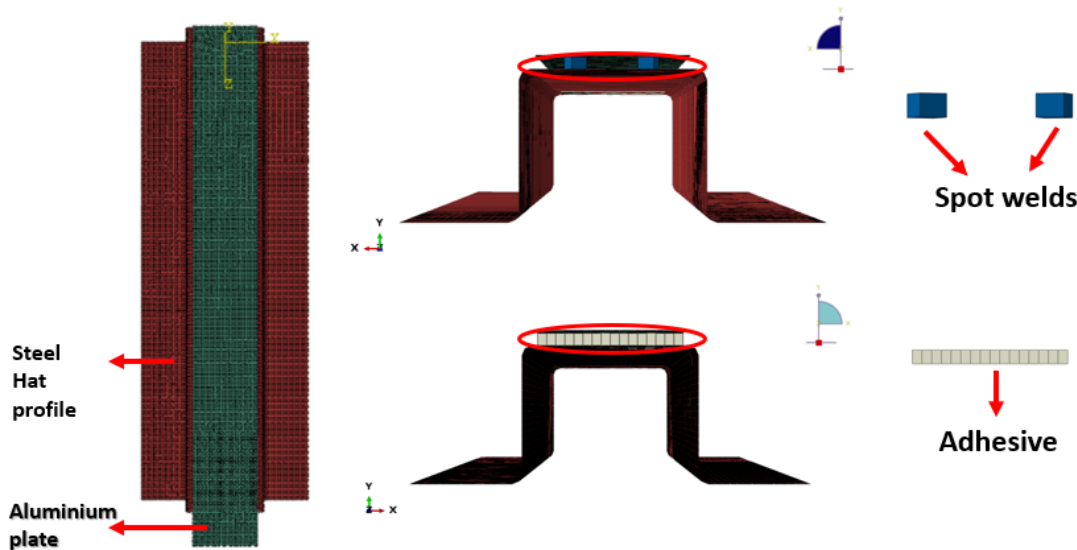


Figure 4.14: Enlarged view of spot welds and adhesive in combined shell model

Table 4.7: Thermal properties used for BETAMATE™ 1480V203

Property	Symbol	Unit	BM1480
Density	$\rho$	ton mm <sup>-3</sup>	1.2e <sup>-9</sup>
Thermal conductivity	$k$	mW mm <sup>-1</sup> K <sup>-1</sup>	2
Specific heat capacity	$c$	mJ ton <sup>-1</sup> K <sup>-1</sup>	1.2e <sup>9</sup>

elastic behavior initially, then crack initiation and followed by continuous crack growth. The elastic behavior relates a normal stress and two local stress components. The values were obtained from experiments directly [8]. The elastic parameters defined by traction separation law used for the adhesive is shown in the Table 4.8 .

Table 4.8: Elastic properties used for BETAMATE™ 1480V203

Elastic modulus normal direction [MPa]	Shear modulus I [MPa]	Shear modulus II [MPa]	Temperature [°C]
1572	492.25	492.25	23
1319.39	306.46	306.46	65
808.59	15	15	110
199.16	4.85	4.85	130
157.83	4	4	150
103.56	2.8	2.8	180

The thermal expansion coefficients for the adhesive is based on the research project [23] and it is listed in the in Table 4.9 . The elastic, damage initiation and damage evolution properties of the adhesive are based on temperature. So, the thermal

expansion coefficients are also defined by interpolation based on temperature.

Table 4.9: Thermal expansion coefficients used for BETAMATE™ 1480V203

<b>Thermal expansion coefficient</b> [ $10^{-4}\text{K}^{-1}$ ]	<b>Temperature</b> [°C]
2.28	23
3	115
3.65	160
4	180

The damage properties of the adhesive is defined by the traction seperation law using quadratic stress criterion (QUADS damage) where the damage is assumed to initiate when the quadratic function involving the stress ratios reaches a value of one. This serves the purpose of calculation of crack initiation. The damage initiation criterion properties are illustrated in the Table 4.10 .

Table 4.10: Damage initiation properties used for BETAMATE™ 1480V203

<b>Nominal stress</b> <b>Normal-only mode</b> [MPa]	<b>Nominal stress</b> <b>first direction</b> [MPa]	<b>Nominal stress</b> <b>second direction</b> [MPa]	<b>Temperature</b> [°C]
33.3	38.32	38.32	23
25.69	27.89	27.89	65
13.59	15.98	15.98	110
4.67	5.42	5.42	130
2.7	3	3	150
1.6	1.55	1.55	180

The damage evolution is modeled using mixed mode behavior and uses a linear approach with maximum degradation [8]. The damage evolution properties are shown in the Table 4.11 .

Table 4.11: Damage evolution properties used for BETAMATE™ 1480V203

<b>Normal mode</b> <b>Fracture energy</b> [ $\text{mJ/mm}^{-2}$ ]	<b>Shear mode I</b> <b>Fracture energy</b> [ $\text{mJ/mm}^{-2}$ ]	<b>Shear mode I</b> <b>Fracture energy</b> [ $\text{mJ/mm}^{-2}$ ]	<b>Temperature</b> [°C]
3.36	8.63	8.63	23
2.96	6.61	6.61	65
2.4	3.85	3.85	110
1.06	1.63	1.63	130
0.19	0.52	0.52	150
0.07	0.2	0.2	180

### 4.3.3 Thermal analysis of combined shell model

This section deals with the thermal analysis of the combined profile to figure out a procedure and the same can be applied for the heat transfer analysis of the Toyota Camry model.

- **Part**

Once the preprocessing of the model is finished in ANSA™, the input file can be generated by clicking **File** → **Output** → **ABAQUS™**. The ABAQUS™ output parameters in ANSA™ must be taken care of. The model version which needs to be output should be mentioned in output format and the output should be of type **Model**. The input file is opened in Abaqus™/CAE by clicking **File** → **Import** → **Model** so that the corresponding input file will be opened in Abaqus™/CAE.

- **Property**

The thermal properties such as Density, Specific heat capacity and Thermal conductivity for Steel, Aluminium and adhesive as mentioned in Tables 4.2, 4.5, 4.7 correspondingly should be used. The thermal properties for spot weld elements should be used the same as Steel material properties. A solid section for the cohesive elements should be created and assigned in this module since ABAQUS™ does not offer heat transfer through cohesive elements.

- **Assembly**

The assembly module can be skipped as the geometry is already assembled and imported from ANSA™ preprocessor.

- **Step**

In this module, a transient heat transfer step should be created with a time period of 2400 seconds. The maximum allowable temperature increment can be changed depending on the user requirement. Usually, it must be a greater value to ensure convergence. In the field output, the nodal temperatures (NT) can be requested as output for the thermal analysis.

- **Interaction**

The Interaction module is the important section where numerous things has to be considered carefully. In the first step, the rigid body constraints should be suppressed, as the element type with only temperature degrees of freedom are allowed in a thermal analysis. This should be done so that the processing of input file is

successful once a job is submitted.

In the next step a temperature-dependent film condition should be defined for both Steel and Aluminium based on the properties from the Tables 4.4 and 4.6 respectively. After the film condition interaction property definition, it has to be assigned to the surfaces of Steel and Aluminium as demonstrated (see Section 3.1.3) With this the temperature-dependent film coefficients can be assigned to the Steel and Aluminium parts of the combined shell model. The cohesive elements represented as solid heat transfer elements and the spot welds are connected to the Steel and Aluminium parts by means of \*TIED contact.

### • Load

To start with the load definition, an initial condition of 180 °C should be applied as a thermal load for the model. This can be achieved by defining a predefined temperature field all over the model.

### • Mesh

The heat transfer shell element types such as DS4, DS3 and solid element type DC3D8 has to be assigned for Steel, Aluminium and adhesive, spot weld elements appropriately. A brief description of the element types is summarized in the Table 4.12 .

Table 4.12: Heat transfer element types used for combined shell model

Element label	Element type	Assigned to	Element description
DS4	Thin shell element	Steel and Aluminium	A 4-node heat transfer quadrilateral shell
DS3	Thin shell element	Steel and Aluminium	A 3-node heat transfer quadrilateral shell
DC3D8	3D heat transfer element	Spot weld and Adhesive	An 8-node linear heat transfer brick

### • Job

In this module, a job should be created and submitted. A successful completion of the job is ensured if all the above steps are done properly. The mechanical analysis of the combined shell model is discussed in detail in the next section.

### 4.3.4 Mechanical analysis of combined shell model

#### Part

The part definition involves the same procedure as explained in (see Section 4.3.3). There is another way of doing the part definition in Abaqus™/CAE. It can be done by right clicking the model in the model tree and copy model.

#### Property

The thermal expansion properties for Steel, Aluminium and adhesive should be used from the Tables 2.1 and 4.9 correspondingly. The thermal expansion for the spot welds is taken same as that of the adhesive so as to prevent the local stiffness degradation in the adhesive due to thermal expansion of the spot welds. The value of coefficient of thermal expansion used for the spot welds is 0.0004 per Kelvin.

The elastic and plastic properties for Steel and Aluminium should be used as shown in the Tables 4.13 - 4.15 respectively. The elastic and plastic properties for Steel and Aluminium are validated with data from tensile tests according to DIN EN ISO 527. The elastic, damage initiation criterion and damage evolution properties for the adhesive should be used as mentioned in the Tables 4.8, 4.10 and 4.11 .

Table 4.13: Elastic properties of DC01 Steel and EN AW-6082-T6 Aluminium

Material	Young's modulus [MPa]	Poisson ratio [-]
Steel	200000	0.3
Aluminium	69000	0.3

Table 4.14: Plastic properties for DC01 Steel

Yield stress [N/mm <sup>2</sup> ]	Plastic strain [-]
255	0
286.875	0.025
308.75	0.047
340.625	0.093
352.5	0.117
364.375	0.14
367.25	0.187
383.125	0.233
390	0.28

The adhesive property section should be reassigned with cohesive elements again since it had been changed to solid heat transfer elements in thermal analysis. The

Table 4.15: Plastic properties for EN AW-6082-T6 Aluminium

<b>Yield stress</b> [N/mm <sup>2</sup> ]	<b>Plastic strain</b> [-]
290	0
308	0.01
322	0.02
328	0.03
334	0.04
340	0.05
345	0.06
350	0.07
354	0.08
358	0.09
363	0.1
367	0.11
371	0.12
373	0.13
377	1

thickness of the cohesive section should be specified using the option **Specify** from the section manager based upon the thickness of the adhesive.

## Assembly

The assembly module can be skipped as the geometry is already assembled and imported from ANSA™ preprocessor.

## Step

In this module a static,general step should be created with a time period of 2400 seconds. The stabilization factor such as dissipated energy fraction is defined with a value of 0.2 and corresponding strain energy value of 0.05 . The initial and maximum time increment values depends upon the user. In the field output, the output variables such as von Mises stress (S), Total strain components (E), Plastic strain components (PE), Displacements (U), Scalar stiffness degradation (SDEG), Damage Initiation criteria (DMICRT) and Status variables (STATUS) are requested. The frequency of the output is made as 40 to reduce the file size of the mechanical analysis output database.

## Interaction

The rigid bodies which are suppressed in the constraint option during the heat transfer analysis should be defined again. If the model is copied from the thermal analysis

using copy option from model tree, the film interaction properties should be deleted as it is not needed for the mechanical analysis.

## Load

A predefined field should be defined with the (.odb) results file from the thermal analysis to apply the nodal temperatures as load for the mechanical analysis.

## Mesh

The shell element types such as S4R, S3R for Steel and Aluminium parts, solid element C3D8 for the spot weld and cohesive element COH3D8 for the adhesive should be assigned respectively. A brief description of the element types used in the mechanical analysis is summarized in the Table 4.16 .

Table 4.16: Stress element types used for combined shell model

Element label	Element type	Assigned to	Element description
S4R	Thin shell element	Steel and Aluminium	A 4-node element, reduced integration, finite membrane strains.
S3R	Thin shell element	Steel and Aluminium	A 3-node element, reduced integration, finite membrane strains.
C3D8	3D continuum element	Spot weld	An 8-node linear heat transfer brick
COH3D8	Cohesive element	Adhesive	An 8-node three-dimensional cohesive element

A damping factor for the cohesive elements can be mentioned if desired. The value used in the mechanical analysis is 0.02 .

## Job

In this module a job can be created and submitted for the mechanical analysis. There might be some convergence issues which has to be dealt with. It is reviewed precisely in Chapter 7 .

In this chapter, a method is identified for simulating the thermal and subsequent structural analysis for the combined shell model by using the validated material properties for Steel, Aluminium and adhesive. This should be employed for the Toyota Camry model to locate the regions where the stresses are high in the adhesive layer. This is dissertated in Chapter 5.

# 5 FEM simulation on the vehicle model

In this chapter, the findings from the validation studies on the Steel and Aluminium materials along with the combined shell model (see Section 4.3) are transferred to a bonded multi-material structure in an overall vehicle body. A description of the vehicle model is clarified in the beginning followed by the part specific detailing and the simulations done for the Toyota Camry model.

## 5.1 Description of the model

An example of the Toyota Camry model examines a hybrid joined aluminium floor panel members on a steel platform with regard to the adhesive connection. The different thermal expansions of the Steel platform and Aluminium floor panel members during the adhesive crosslinking in the paint drying process causes the floor panel members to slide over the platform. This might lead to deformations in the flange and relevant stresses in the adhesive layer during cooling. This should be analyzed based upon the simulation results which will be discussed in the subsequent chapter (see Chapter 6).

## 5.2 Brief discussion on Toyota Camry model

A FE model of the Toyota Camry whose body is made up of shell elements is used to calculate the flange deformations and their impact on the strength of the adhesive bond. The body panels are made up of shell element types S4R and S3R. The aluminium (EN AW-6082-T6, thickness: 3.5mm) floor panel members has the material definition (see Tables 2.1, 4.13, 4.15) for mechanical analysis. The floor platform (DC01, thickness: 0.75mm) and other sheet metal parts are made up of Steel and has the material definition (see Tables 2.1, 4.13, 4.14). The 0.3mm thick adhesive layer represented by cohesive elements is defined by damage model by traction seperation law. The adhesive has material definition properties as mentioned in Tables 4.8 - 4.11. The aluminium flanges which is fixed to the steel platform is illustrated in Figures 5.1 - 5.2 .

The FE representation of the adhesive elements defined by traction seperation law are cohesive elements in ABAQUS™. The cohesive element depicted in Figure 5.3 gives the idea about how it is modeled in the vehicle structure as well the combined shell model (see Section 4.3.1). It is a 3D-element with top and bottom faces along

the thickness direction. The cohesive zone is present in the middle surface and it is discretized with single layer of cohesive elements through the thickness.

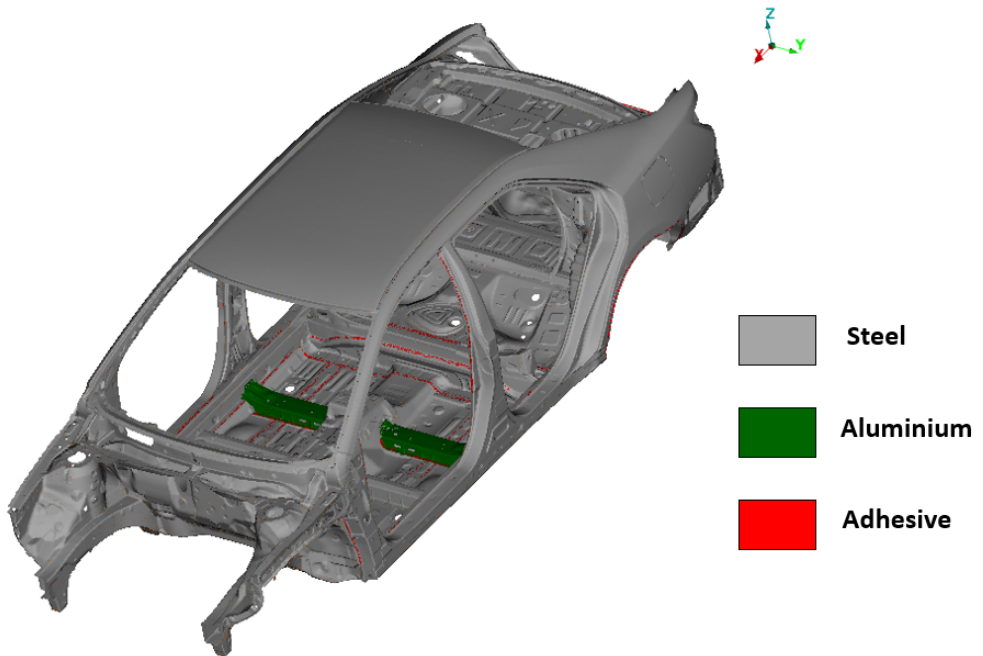


Figure 5.1: Aluminium parts in the entire car model

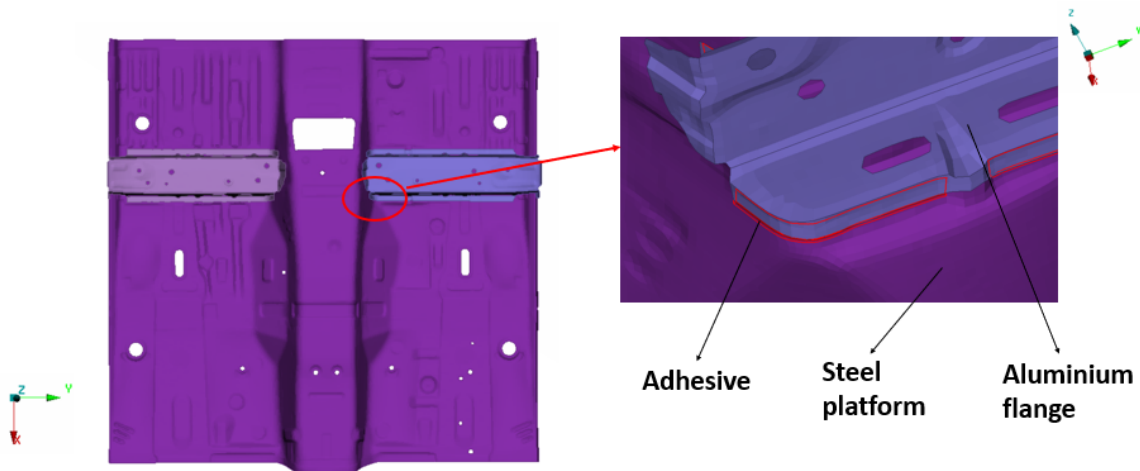


Figure 5.2: Aluminium flanges glued to the Steel platform

The similar FE representation of the PAM-CRASH™ COS3D element represented in the Figure 5.3 is the cohesive element of type COH3D8 in ABAQUS™.

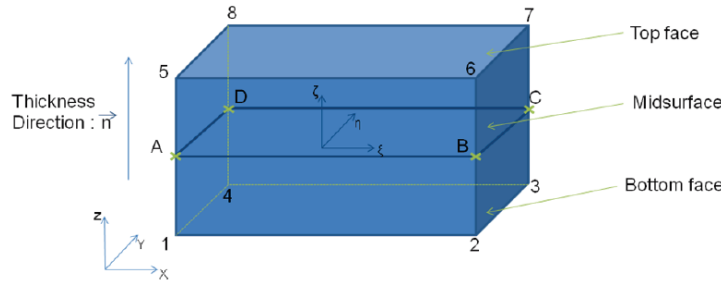


Figure 5.3: Cohesive element type COS3D in PAM-CRASH™ [5]

## 5.3 Thermal and Mechanical analysis of the vehicle structure

This section describes the thermal and mechanical analysis of the Toyota Camry model. The thermal analysis is carried out in the same procedure (see Section 4.3.3) like the combined shell model. An initial condition of  $180^{\circ}\text{C}$  is applied as a thermal load. The film condition interaction properties for the Steel and Aluminium parts are defined as summarized in the Tables 4.4 and 4.6. The model is allowed to cool down to room temperature of  $23^{\circ}\text{C}$ . The nodal temperatures which are obtained as a result of the transient heat transfer analysis are inhomogenous. Since the shell parts are of different thickness, each part has a different cooling rate when compared to the other. This can be seen by measuring the temperatures at various points. It reflects the real temperature distribution in the BIW structure with sufficient accuracy.

The successive mechanical analysis is done using the results from the transient thermal analysis. The mechanical analysis is done in two ways. The first one is by including only the elastic properties with the coefficient of thermal expansion for Steel, Aluminium, adhesive and spotwelds. The second one is with both elastic and plastic properties with the coefficient of thermal expansion. The stabilization factor is applied as described in Section 4.3.4 . The nodal temperatures are applied as a load using the predefined temperature field option. The rigid body constraints which are already present in the model are activated again so as to provide rigid body motion in certain regions. No boundary conditions or fixtures are applied to the model. The frequency of the output is made as 80 to reduce the file size. Both the thermal and mechanical simulations are allowed to run for a time period of 2400 seconds. The element types for both simulations are assigned according to the Tables 4.12 and 4.16 .

Up to now, the introduction to the problems, workflow and the FE simulation using the validated material properties is adapted to notice the damage in the bonding regions of adhesives. The results of the analysis is analyzed in Chapter 6 and some controlling measures has to be decided based upon them.

# 6 Observation and Results

Initially the results of the heat transfer analysis is explained. The temperature distribution and the temperature differences of the parts are examined. Figure 6.1 shows the temperature distribution during the cool down process of the Camry model after a time period of 527 seconds.

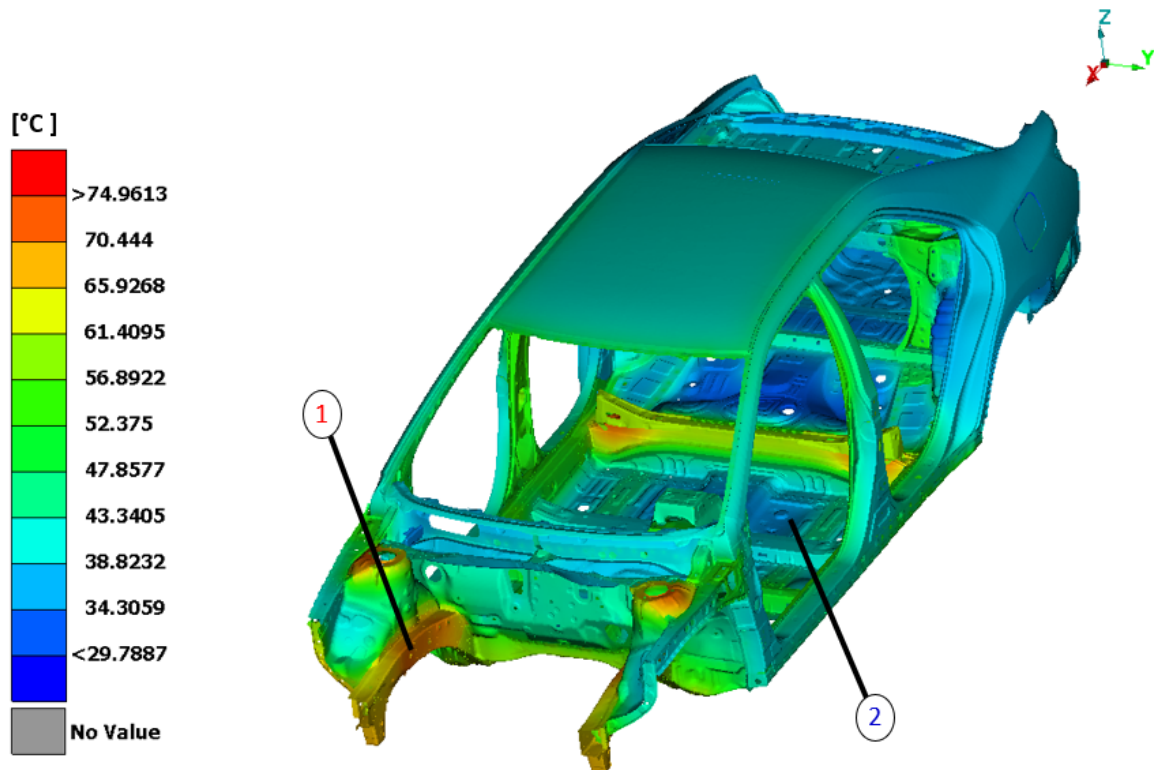


Figure 6.1: Temperature distribution after 527 seconds during cooling

It can be observed that part 1 right midrail (thickness = 2.628mm) of the model is still warm at 71 °C while the other part 2 floor front (thickness = 0.75mm) is at 45 °C. The reason for this difference is the variation in the thickness of the components and geometry. The variations in temperatures is represented in the Figure 6.2. The temperature distribution is inhomogenous which means that a temperature is assigned to each node N at a specific time period 't' [7]. The temperature differences in the parts connected by spot welds is also analyzed. To know about the changes in temperatures specifically, a region of the model is verified. For example, the upper rail in Figure 6.3 is present in the front part of the car model and chosen for investigation. The nodal temperature differences of both parts connected by spot weld are plotted for the entire time period and is shown in Figure 6.4. The region marked in red circle in Figure 6.3 displays the measurement point at which the temperatures are recorded. The element which is represented in brown color inside the circle is the spot weld to conduct heat transfer between the components.

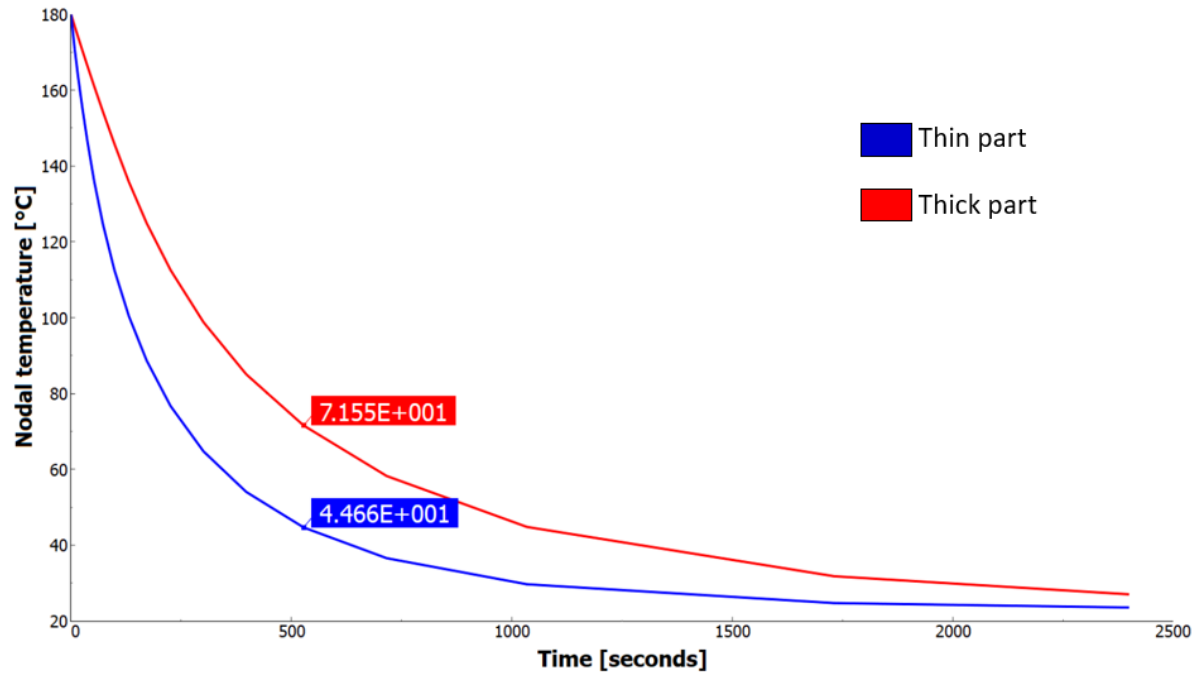


Figure 6.2: Temperature difference between thick and thin shell parts

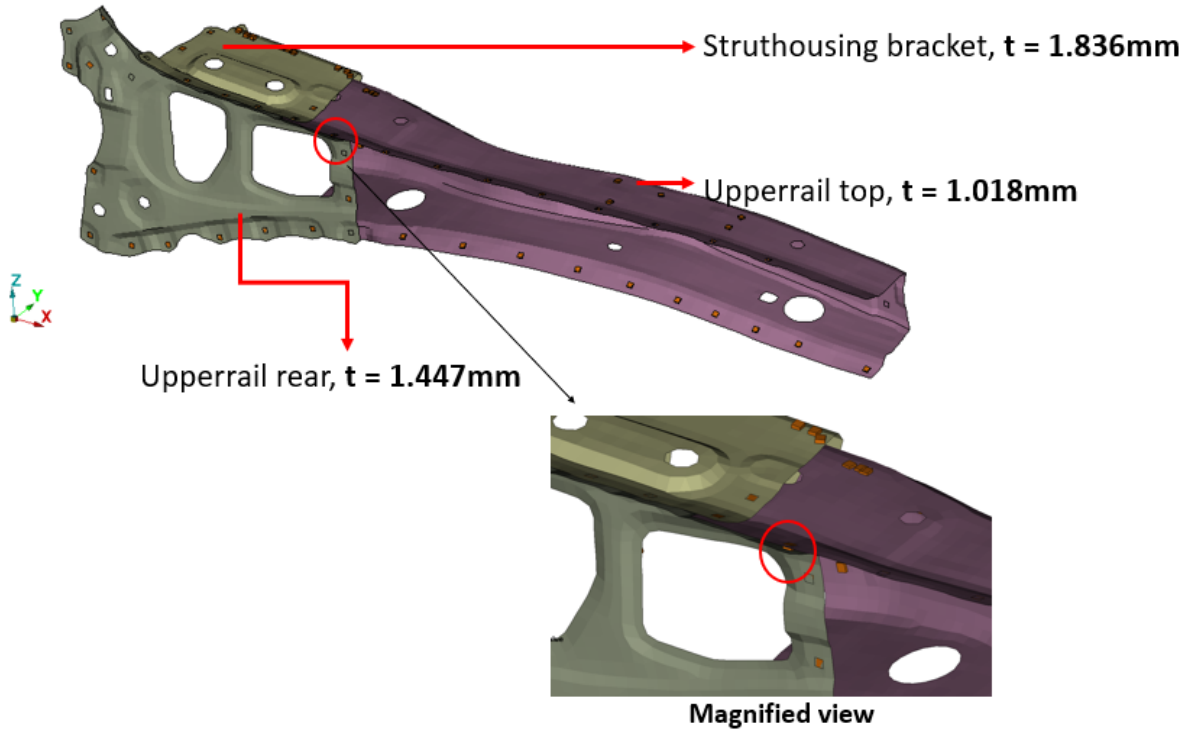


Figure 6.3: Measurement point to illustrate temperature difference

From the Figure 6.4 , it is noticed that the blue and the red lines are almost coincident with each other. This means that there is a mild difference of about 1 ° C over 2400

seconds and it can also be seen from the labels inside the image.

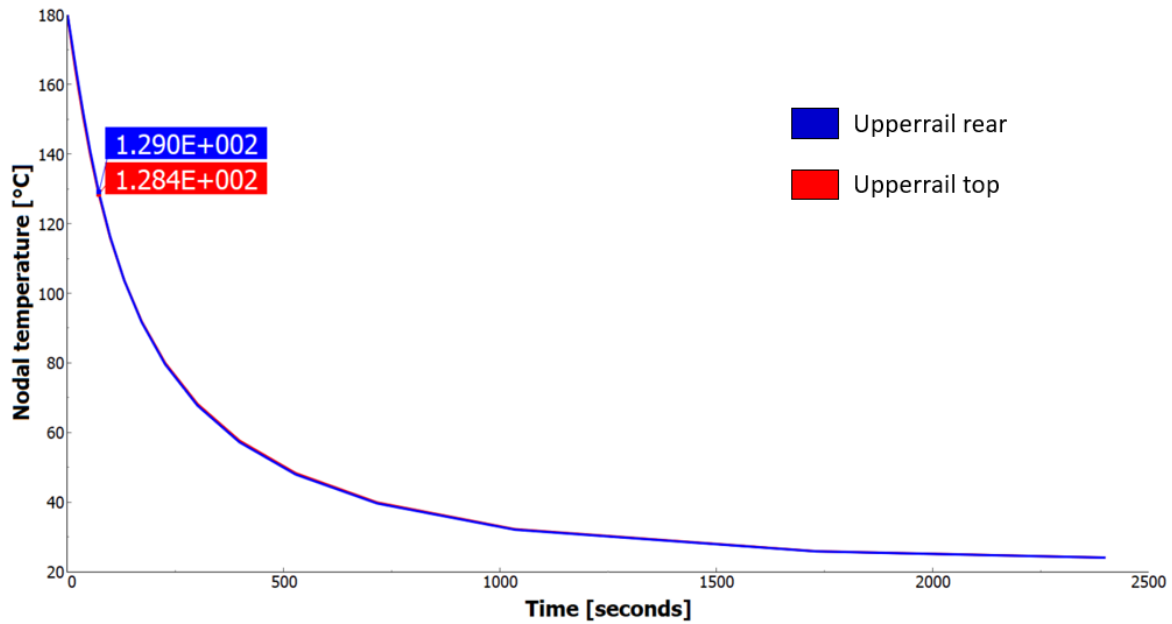


Figure 6.4: Temperature difference of upper rail rear and top parts connected by spotweld

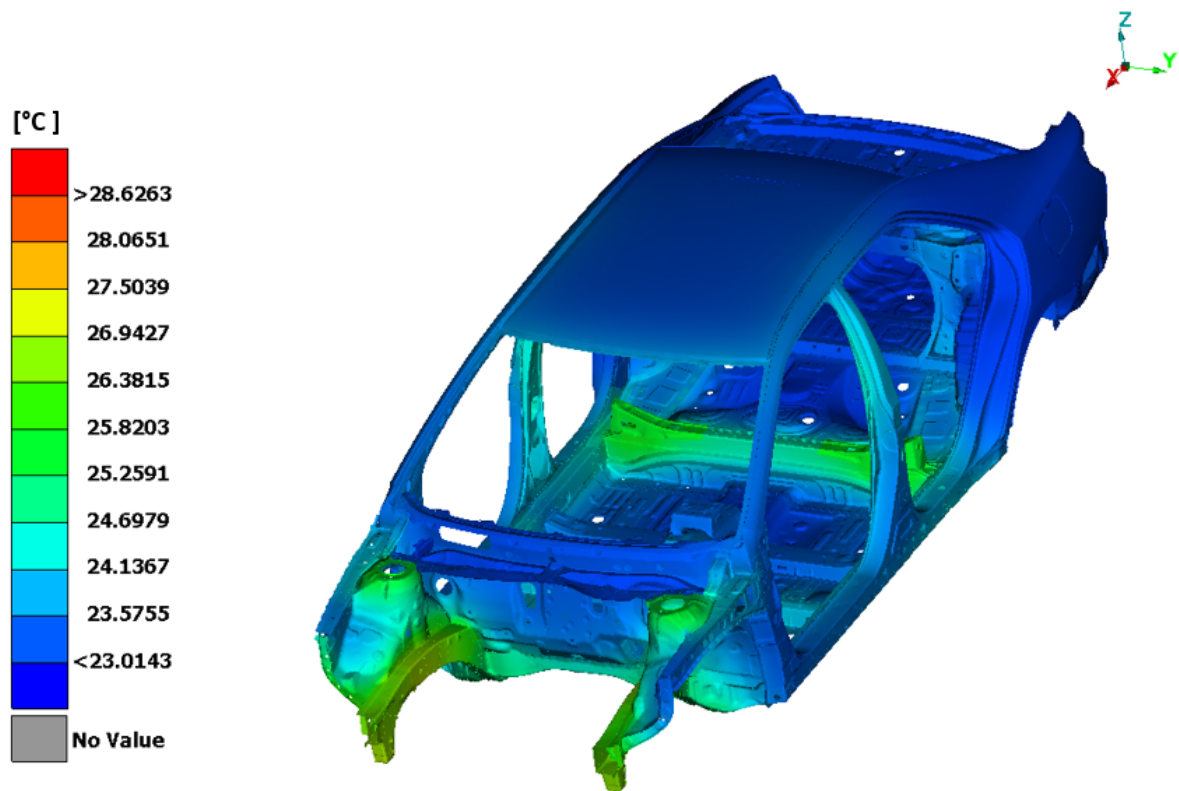


Figure 6.5: Temperature distribution of Camry model after 2400 seconds

---

## 6 Observation and Results

---

This difference is indeed reasonable and precisely accurate to the real model which is being used in the CDP paint drying oven. The temperature distribution of the model after a time period of 2400 seconds is shown in the Figure 6.5 . It is noticed that some of the parts have not reached the room temperature 23° C. But the difference is not so high and it is accepted to use the thermal analysis results for the structural simulation.

The structural analysis as quoted earlier, is done in two ways. The approximate extent of the mechanical analysis simulated in ABAQUS™ is illustrated in the Table 6.1 . The mechanical simulation with elastic properties aborted after a time period of 925 seconds due to convergence issues. But this is of limited concern in the stated problem because practically under thermal loads the nominal stress of the material can exceed the yield stress. Hence, the results from the mechanical analysis which includes the plasticity material properties is analyzed in this part.

Table 6.1: Comparative time duration of the analysis jobs

<b>Analysis</b>	<b>Time duration</b>	<b>Status</b>
Thermal	4 to 5 hours	Completed
Mechanical with elastic properties	15 to 18 hours	Aborted
Mechanical with both properties	140 hours	Completed 438 seconds(Still running)

Eventhough the mechanical simulation with plastic properties does not have convergency problems, the computation time is really slow. This leads to the prolonged running time of the analysis. To complete a time period of 280 seconds in the simulation, 96 hours of running time is required (Direct solver with 8 processors). The analysis results are therefore discussed at a time step of 280 seconds. The overall magnitude of the displacements after 280 seconds in the Camry model is presented in the Figure 6.6 . Some parts of the Camry model to name a few such as the roof cross members and the console base are not properly connected to the neighbouring components. These concerns are also reasons for the slower computational effort. As this is a cool down procedure, the adhesive is fully cured at this point and the relative displacements will start to decrease [8]. A maximum summed up displacement of 6 to 8mm is identified in the roof cross members. An overall peak displacement of magnitude 4mm is spotted in the entire body. Figure 6.7 scaled by a factor of 5 shows the calculated permanent deformation of the floor front in the z,x-directions respectively. During cooling the entire vehicle starts to contract and hence the floor front connected to the rear floor panel and firewall by means of spot weld and adhesive displaces about 0.4mm along x-direction on both sides and is illustrated in the right side of the figure. This in turn leads to the buckling of certain regions along the z-direction which is displayed in the left side. A maximum displacement of about

2mm is found in the z-direction.

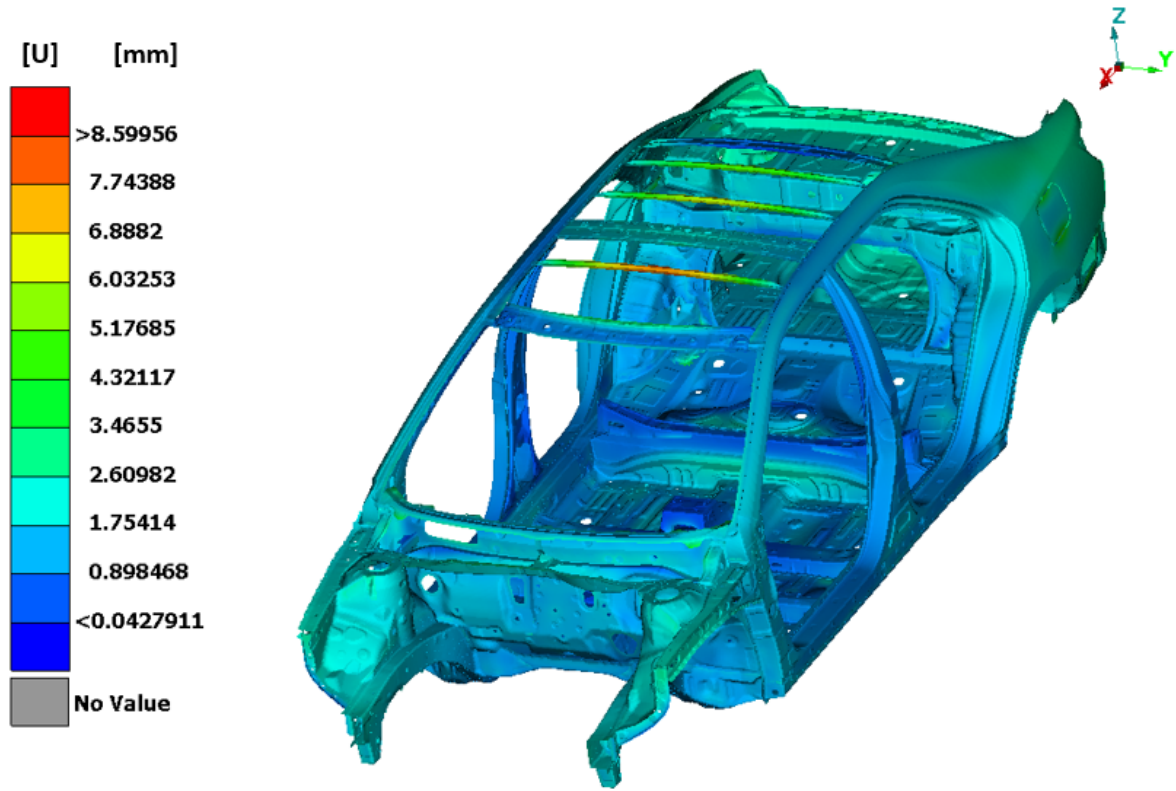


Figure 6.6: Displacement of the Camry model after 280 seconds

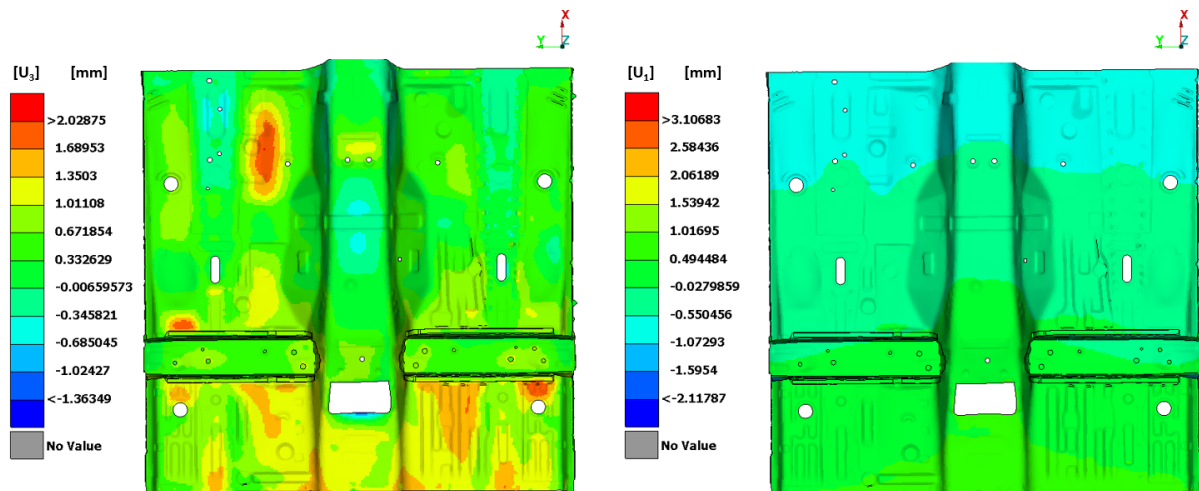


Figure 6.7: Displacement of the floor front during cooling

This acts as a cause for the parts connected to the floor front to move along the z-direction. The aluminium flange connected to the floor front by adhesive is allowed to move only in the middle region since the ends are attached to the rocker panels

by means of spot weld. In addition to this, the higher thermal expansion coefficient of the aluminium flange than the steel leads to further shift from its position.

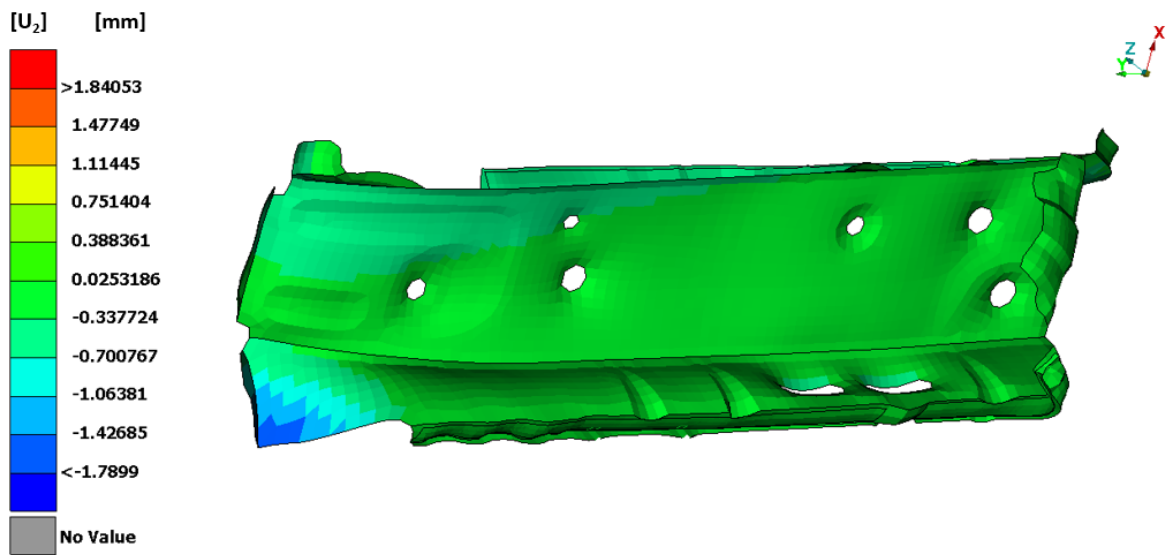


Figure 6.8: Deformation of the aluminium flange

From Figure 6.8 scaled by a factor of 20, it is seen that the flanges undergo compression along the y-direction of about 1mm since it is firmly fixed to the rocker panels and also have a pulling effect on the adhesive and displaces about 0.2mm in z-direction due to the contraction of floor front along x-direction. This paves the way for the degradation in the stiffness of the adhesive layer. In ABAQUS™ there is a possibility of element deletion based upon damage or the stiffness degradation. The default value of maximum degradation is 1 upon which no stresses will be accumulated in the integration point and removal of element happens as an aftereffect. The stiffness degradation of the adhesive in certain regions are discussed in this part. The two regions such as B-pillar and the rear outer panel near the trunk floor are examined.

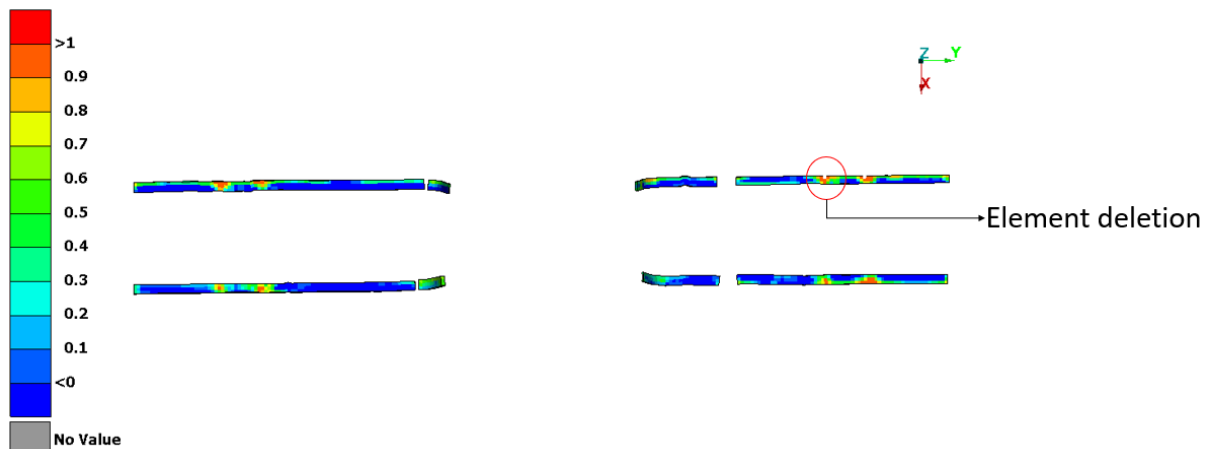


Figure 6.9: Stiffness degradation of the adhesive in region of aluminium flange

Before conferring about the above acknowledged two regions, initially the firmness of the adhesive in the aluminium flange (depicted in Figure 6.9) is reviewed. It is seen that in the mid-region of the adhesive marked in red circle, the degradation is maximum. This happens because the adhesive which glues the floor front rear support crosses this region and a spot weld (shown in circles in Figure 6.10) within the glue is present right beneath the adhesive region associated with flanges. The whole of the floor front shrinks and therefore the other regions of the adhesive correlated with aluminum flanges shows significant stiffness degradation.

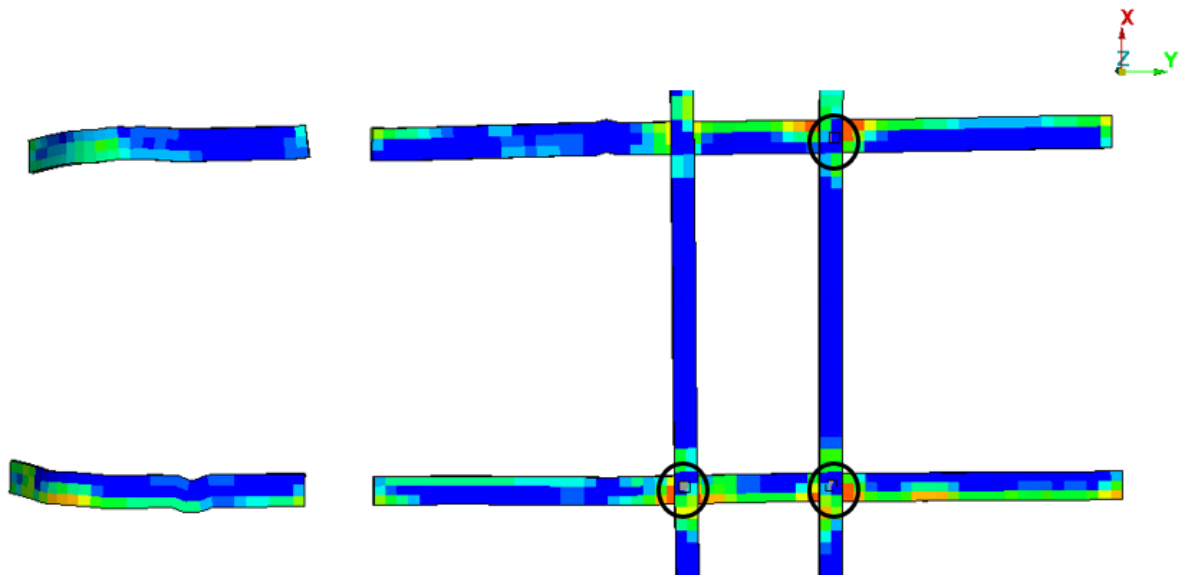


Figure 6.10: Crossing of adhesives with spot weld

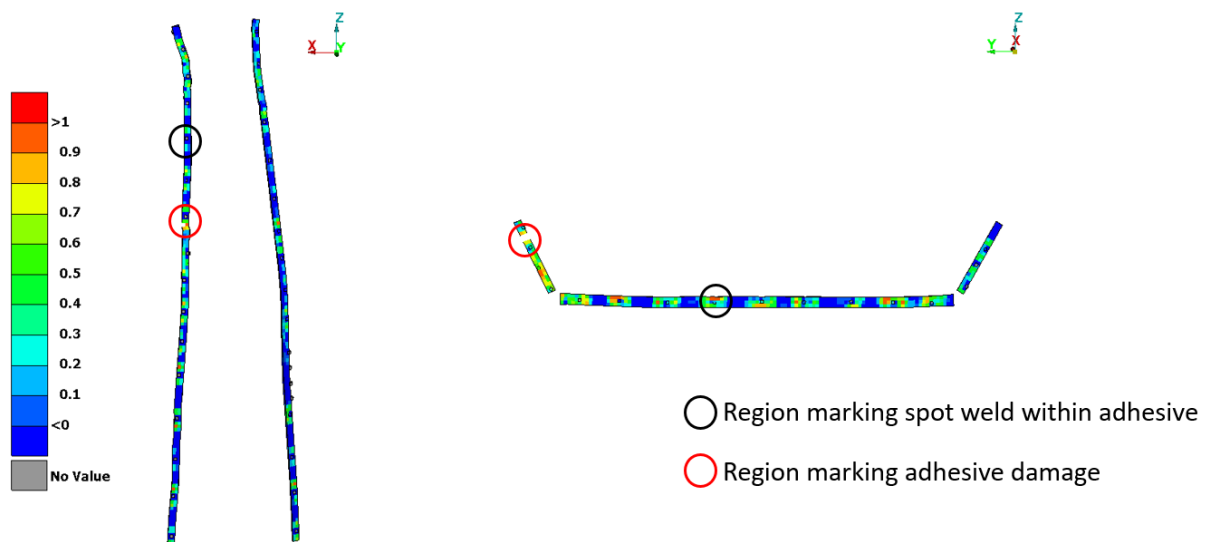


Figure 6.11: SDEG results in B-pillar and rear outer panel

The glue which joins the B-pillar with the side panel and the rear outer panel which

abuts the trunk floor has some effects due to cooling and is presented in the Figure 6.11 . In reality, in region of the spot weld within the adhesive, there will be minimal or no degradation in the gummy. The results which is obtained also resembles the same in areas of B-pillar (marked in black circle) displayed in left side of the figure. But this is not the case in the rear outer panel because it displaces to a considerably greater extent which has a squeezing effect on the adhesive glued to the trunk floor. So there occurs minimum reduction in the stiffness in spot weld regions within adhesive. There is also element deletion (marked in red circle) and this is due to the reason of a gap opening due to a displacement of 1mm along the y-direction from the inner side of B-pillar towards the side panel. Due to the compression of the rear outer panel towards the trunk floor of about 2.5mm in x-direction there appears adhesive damage represented in right side of figure.

Further, there are also some components associated with adhesive which have to be considered as critical spots. They are listed below:

- Roof outer panel
- Wheel housing
- Floor front

Thus far the component displacement and the reduction in adhesive stiffness is investigated in the Camry model. A way should be explored to know why the process time is high. The threats which are defied during the pre-processing and analysis stages are considered in detail in Chapter 7.

# 7 Objections confronted

This chapter works out on the challenges which are encountered during the modeling and the simulation phases briefly. This will serve as a heads-up if any problem comes up in the future regarding this work.

The three main issues which has to be considered in detail are:

- Model redefinition
- Convergence issues
- Post-processing results

The first point which deals with the model redefinition is concerning the doors and flaps in the Toyota Camry model. Usually, the body in white represents the body along with the doors and flaps. But in this work, the doors and flaps are removed. The reason behind this is, the model which is elaborated in this work where the doors and flaps are parts of another assembly and are connected to the body by means of rigid body constraints or MPC constraints. When the body with doors and flaps are included in the mechanical analysis, due to the thermal expansion in the elements of the doors and flaps it tends to distort excessively. This leads to the convergence problems. So, in order to discover the stresses in the adhesive which is present in the body of the model, the doors and flaps are removed so that it might not affect the results. But for future works it is important to find another way to connect the doors and flaps to the body, because for the CDP process the entire BIW should be considered.

After removing the doors and flaps, some convergence problems still existed. This can be overcome by using the **Discontinuous** analysis option in the structural analysis. Normally, FEM programs use default values to control the Newton iterations. If no convergence is reached after a fixed number of iterations, then the time step is cut-back. So, if the default value is increased which controls the solution technique, then the convergency problems can be solved to some extent [24]. In the Step module, the discontinuous analysis can be included in the input file by **Other → General solution controls → Edit → Step**. By clicking the radio-button **Specify** and then in the time incrementation tab, toggle on the Discontinuous analysis option.

There are some erroneous ways in which the analysis results can be interpreted during post-processing. Since the model is made up of shell elements, the stresses or displacements or temperatures are to be analyzed carefully based upon the section points. This is due to the fact that the shell is drafted as a wireframe model in ABAQUS™ and extruded based upon the thickness provided in section manager. In

computational sense, half the thickness is assigned above and half the thickness is assigned below (if the middle surface is the reference surface of the shell) the reference surface. So, it is crucial to look at the section points rather than the same way of post-processing a solid model. This applies to both thermal and structural analysis results. It can be done in the **Visualization** module, select **Result → Section points → Bottom or Top or (both Top and Bottom)**. During the thermal analysis in addition to the nodal temperatures (NT), the temperature variable (TEMP) should be requested to look upon the temperatures based on section points. During the mechanical output database analysis the von Mises stress (S) shows higher values which seems to be odd. This is because the von Mises is always positive component of the stress and displays peak values. The bending stress of the model can only be observed by choosing the suitable stress components such as S11, S22, S33 to know whether it is involving tension or compression and S12, S13 and S23 for the shear stresses. The same technique should also be adapted for analyzing the displacement of the components.

It is important to consider the points which are deliberated above in order to simulate the multi-material BIW structure.

# 8 Summary

The work contributes to locating the critical spots in the adhesive layer in glued multi-material BIW structures. The adhesive undergoes complex mechanical and high thermal stresses during the manufacturing process. So, the mechanical and thermal description of the adhesive plays an important role in the design of the adhesive connections in the vehicle structure. High temperatures during the CDP process not only leads to the adhesive crosslinking but also the thermal expansion of different materials used in the multi-material BIW structures. The method implemented in this work can be used for numerical calculations of the permanent deformations and also the strength of the adhesive layer.

In Chapter 1, the problems experienced during new lightweight construction developments are discussed. A description of the CDC process, adhesive and the goal of the work is presented.

The Chapter 2 involves a brief introduction to the cathodic dip painting process. The adhesives used during the construction of modern BIW is shown and the most important delta alpha problem which happens during the paint-dryer process is reviewed.

The workflow used in this work is summarized in Chapter 3. The design modifications done in ANSA™ preprocessor via the connection manager is explained. The sequentially coupled thermal-stress analysis is elaborated step-by-step to get an understanding of the process that is to be done in ABAQUS™.

The Chapter 4 carried out the validation for the material models to obtain the temperature-dependent film coefficient properties to be used in the thermal analysis of the vehicle model. A model where the Steel and Aluminium profiles are connected with each other by means of an adhesive and spot welds is also made clear to know about the procedure for applying it to the Toyota Camry model.

In Chapter 5, a description about the glued BIW structure is given. The thermal expansion behavior of the Aluminium flanges adhered to the Steel platform is a perfect example to know about the delta alpha problem and it is examined. The thermal and mechanical analysis of the Toyota Camry model done in ABAQUS™ is discussed.

The stiffness degradation of the adhesives used in the Toyota camry model is conferred in Chapter 6. The resulting displacements of the model as a result of the thermal analysis is evaluated to know more about the deformations that can happen during the paint drying process.

The Chapter 7 comes across the challenges that are faced during the modeling phase in ANSA™ preprocessor and also during the simulation phase in ABAQUS™.

In relation to the previous works based on this topic, the calculation method described in this work offers another possibility such as the heat transfer through the spot welds in thermal analysis. For a future application of the method in the automotive industries, a experimental verification of the glued BIW structure numerically calculated in this work is desirable. It should also be noted that a criterion should be evaluated for the permissible stress in the adhesive layer and applied to other adhesives as well.

# 9 Bibliography

- [1] KTL Beschichtung, BASF Coatings. URL <https://www.bASF-coatings.com/global/ecweb/de/content/press/coatings-partner-magazine/archive/automotive-oem-coatings/ein-lack-geht-um-die-welt>.
- [2] Cathodic dip paint dryer. URL <https://www.durr.com/de/produkte/lackieranlagen-applikationstechnik/trockner/>.
- [3] Cornelis Wirth. *Berechnungskonzept für die Klebflanschfestigkeit in Gesamtkarosseriemodellen*. PhD thesis, Technische Universität München, Germany, 2004.
- [4] BETA CAE systems, ANSA User guide 2019 version 19.1.2.
- [5] ESI Group, PAM-CRASH 2015 Solver Reference Manual.
- [6] EU Kommission: Questions and answers on the proposed regulation to reduce CO<sub>2</sub> emissions from cars. *MEMO/07/597*, 2007. URL [https://ec.europa.eu/commission/presscorner/detail/en/MEMO\\_07\\_597](https://ec.europa.eu/commission/presscorner/detail/en/MEMO_07_597).
- [7] Stephan Menzel. *Zur Berechnung von Klebverbindungen hybrider Karosseriestrukturen beim Lacktrocknungsprozess*. PhD thesis, Technische Universität Dresden, Germany, 2011.
- [8] Niklas Günther, Michael Griese, Elisabeth Stammen, and Klaus Dilger. Modeling of adhesive layers with temperature-dependent cohesive zone elements for predicting adhesive failure during the drying process of cathodic dip painting. *Materials: Design and Applications*, 2018. doi: 10.1177/1464420718806005.
- [9] Electrophoretic deposition. URL [https://de.wikipedia.org/wiki/Elektrophoretische\\_Abscheidung](https://de.wikipedia.org/wiki/Elektrophoretische_Abscheidung).
- [10] Funktionelle Beschichtungen (Korrosionsschutz/Konservierung/Reinigungsvermeidung). URL [http://cec-leonberg.de/cleanwiki/index.php/Funktionelle\\_Beschichtungen\\_\(Korrosionsschutz/Konservierung/Reinigungsvermeidung\)](http://cec-leonberg.de/cleanwiki/index.php/Funktionelle_Beschichtungen_(Korrosionsschutz/Konservierung/Reinigungsvermeidung)).
- [11] Laxmidhar Besra and Meilin Liu. A review on fundamentals and applications of electrophoretic deposition (epd). 2006. doi: 10.1016/j.jpmatsci.2006.07.001. URL <https://www.sciencedirect.com/science/article/pii/S0079642506000387>.
- [12] Cathodic dip painting. URL [http://www.chemgapedia.de/vsengine/vlu/vsc/de/ch/9/mac/netzwerke/lacke/eltauch.vscml.html](http://www.chemgapedia.de/vsengine/vlu/vsc/de/ch/9/mac/netzwerke/lacke/autolack.vlu/Page/vsc/de/ch/9/mac/netzwerke/lacke/eltauch.vscml.html).

- [13] Ralf Albrecht, Paul Buschke, and Weiwei Zhang. Ultraschallprüfung von klebeverbindungen im automobil-karosseriebau. *DGZfP JahresTagung*, 2017. URL <https://www.ndt.net/search/docs.php3?showForm=off&id=21401>.
- [14] Robert Georg Dietrich. *Analyse der Wärmeausdehnungs-Inkompatibilität bei Klebverbindungen aus CFK, Stahl und Aluminium bei der Fertigung einer lackierten Karosserie*. PhD thesis, Technische Universität München, Germany, 2017.
- [15] Gerd Habenicht. *Kleben: Grundlagen, Technologien, Anwendungen, 6<sup>th</sup> Edition*. Springer publishing company, 2009.
- [16] B Hüsgen. *Beitrag zum Einfluß der Fertigung auf ausgewählte Eigenschaften von Klebverbindungen mit warmaushärtenden Klebstoffen*. PhD thesis, Paderborn, Germany, 1993.
- [17] Numerische abschätzung von eigenspannungen und bauteilverformungen in gesamtfahrzeugmodellen beim kleben im karosseriebau. *Paderborner Symposium Fügetechnik*, 2006. URL [https://www.theses-fe.com/thc\\_content/publications/slides/20061129\\_slides\\_kleben-im-karosseriebau\\_prozess-simulation\\_de.pdf](https://www.theses-fe.com/thc_content/publications/slides/20061129_slides_kleben-im-karosseriebau_prozess-simulation_de.pdf).
- [18] ANSA pre-processor introduction. URL <https://www.beta-cae.com/ansa.htm>.
- [19] SIMULIA Abaqus FEA. . URL <https://en.wikipedia.org/wiki/Abaqus>.
- [20] Dassault systemes® Abaqus/CAE. . URL <https://www.3ds.com/products-services/simulia/products/abaqus/abaquscae/>.
- [21] Sequentially coupled thermal-stress analysis. URL <https://abaqus-docs.mit.edu/2017/English/SIMACAEANLRefMap/simaanl-c-thermstresanal.htm>.
- [22] BETAMATE™ 1480V203 Technical Datasheet. *Dow Europe GmbH, Edition 13.07.10*. URL <https://www.antala.es/Files/tds/Dow%20Automotive/English/TDS%20BETAMATE%201480V203%20-%20english.pdf>.
- [23] Alexander Lion, Anton Matzenmiller, Gerson Meschut, Dominik Teutenberg, Patrick Kühlmeyer, and Christoph Liebl. Development of methods for simulation and evaluation of damage in adhesive layers due to thermal cyclic loadings during manufacturing and operation. *Forschungsvorhaben P878, Förderkennzeichen 369 ZN*, 2014.
- [24] Martin Bäker. How to get meaningful and correct results from your finite element model. *Institut für Werkstoffe, Technische Universität Braunschweig*, 2018. URL [https://www.researchgate.net/publication/328956103\\_How\\_to\\_get\\_meaningful\\_and\\_correct\\_results\\_from\\_your\\_finite\\_element\\_model](https://www.researchgate.net/publication/328956103_How_to_get_meaningful_and_correct_results_from_your_finite_element_model).